Research Square

Preprints are preliminary reports that have not undergone peer review.
They should not be considered conclusive, used to inform clinical practice,
or referenced by the media as validated information.

# Breeding of high-yield low-temperature lipase fungi, optimization of fermentation conditions and isolation and purification of lipase

**Lutong Yang**
East University Of Heilongjiang
**Mengai Wang**
East University Of Heilongjiang
**Hongyan Fu**
East University Of Heilongjiang
**Yun Zhang**
East University Of Heilongjiang
**Yu Zhang**
East University Of Heilongjiang
**Mengni Cui**
East University Of Heilongjiang
**Bowen Jiang**
East University Of Heilongjiang
**Hong Chen**
East University Of Heilongjiang
**Yanwei Cui**
cyw561@sina.com
East University Of Heilongjiang

**Article**

**Keywords:** Low-temperature lipase, Aspergillus niger, Mutagenesis breeding, Fermentation optimization, Lipase properties

**Posted Date:** June 29th, 2026

**DOI:** https://doi.org/10.21203/rs.3.rs-9989697/v1

**License:** This work is licensed under a Creative Commons Attribution 4.0 International License.
Read Full License

**Additional Declarations:** No competing interests reported.

**Version of Record:** A version of this preprint was published at Scientific Reports on October 5th, 2026. See the published version at https://doi.org/10.1038/s41598-026-74081-7.

# Breeding of high-yield low-temperature lipase fungi, optimization of fermentation conditions and isolation and purification of lipase

**Lutong Yang[a], Mengai Wang[a], Hongyan Fu[a], Yun Zhang[a], Yu Zhang[a], Mengni Cui[a], Bowen Jiang[a], Hong Chen[a] and Yanwei Cui[a]***

[1]College of Food Engineering, East University of Heilongjiang, Harbin, 150066, Heilongjiang, China

*Corresponding author E-mail: cyw561@sina.com

## ABSTRACT

The low-temperature lipase, due to its unique low-temperature adaptability and catalytic properties, has become a highly focused research hotspot in the field of enzymology, and the re-search around it has been continuously deepening. This study aims to efficiently produce a low-temperature lipase to address the problems of low activity, high cost, and limited application of common lipases under low-temperature conditions. During the research process, we collected samples from the natural environment at low temperatures, and through multiple rounds of screening, we obtained fungi with strong lipase production capabilities. We further enhanced their lipase production capacity through ultraviolet-uranine guanidine compound mutagenesis and optimization of fermentation conditions. Finally, we separated and purified the lipase using ammonium sulfate precipitation, Q-HP anion exchange chromatography, and Superdex 75 gel filtration chromatography, and determined its Lipaseology properties. The research results showed that a strain of Aspergillus niger was screened out. After mutagenesis treatment, the mutant strain increased the lipase production by 127.35%. On this basis, the lipase production

was further improved to 57.26 U/mL under optimized fermentation conditions. The isolated low-temperature lipase had a specific activity of up to 113.52 U/mg. Its optimal reaction temperature was measured to be 30℃, and it still maintained over 60% activity at 15℃, which was higher than the low-temperature activity of common commercial lipases. The low-temperature lipase obtained in this study can be applied in food processing, low-temperature washing, and environmental governance, effectively reducing the energy consumption and operating costs of related industries. The related preparation methods can provide a scientific basis and feasible solutions for the large-scale production of low-temperature lipases.

**Keywords:** Low-temperature lipase, Aspergillus niger, Mutagenesis breeding, Fermentation optimization, Lipase properties

## Introduction

Lipase belongs to the carboxylester hydrolase class and is capable of gradually hydrolyzing triglycerides into glycerol and fatty acids[1,2]. It is one of the important industrial enzyme preparations, which can catalyze lipidolysis reactions, transesterification reactions, alcoholysis reactions, and ester synthesis reactions[3-5]. It is widely used in the processing of oil and chemical products, food and nutrition, agricultural chemicals, and daily chemicals industries[6]. Lipase from different sources have different catalytic characteristics and activities. Lipase are widely present in nature, including animals, plants, and microorganisms[7,8]. Among them, microbial lipase are the main source of industrial lipase due to their diverse types, rapid reproduction, easy genetic variation, broader pH and temperature ranges of activity, substrate specificity, and generally being secreted extracellular enzymes, which are convenient for industrial production and

obtaining high-purity samples[7,9,10].Qiurun M[11] et al. isolated *Xanthomonas oryzae pv. Oryzae(YB103)* from soil samples as an intracellular thermostable and organic solvent-resistant lipase producer with a lipase specific activity of 373.9 U/mg.

Low-temperature lipases are a special type of lipase that can maintain high catalytic activity under low-temperature conditions (typically below 40℃, with the optimal reaction temperature mostly ranging from 0 to 30℃)[12,13]. They possess characteristics such as high activity at low temperatures, thermal instability, and structural flexibility. These lipases are mainly produced by microorganisms that have long lived in cold environments such as the Antarctic, Arctic, and deep sea, including genera like Pseudomonas, Psychrobacter, and Bacillus[9,13,14].Balaei F[15] et al. site-directed mutagenesis of a *Psychrobacter sp. C18* strain showed that the optimum temperature for lipase in the mutant was reduced to 20℃.

In the research of lipase breeding, traditional mutagenesis breeding technology is an important means to increase the yield and performance of lipase[14]. Through physical mutagenesis (such as ultraviolet rays, gamma rays, etc.) and chemical mutagenesis (such as nitrosoguanidine, etc.) methods, the lipase-producing bacteria can undergo gene mutations, and strains with excellent traits can be screened from a large number of mutants[16,17].Shreya[18] et al. used ethyl mesylate to mutate *Aspergillus eucalypticola CBS 122712*, and finally obtained a mutant strain with lipase activity of 119.05 ± 0.14 IU/ml/min.

This study addresses the challenge posed by traditional lipases, which, owing to their elevated optimal catalytic temperatures, often induce substrate inactivation and product degradation during the processing of heat-sensitive substances, consequently resulting in diminished biotransformation efficiency and compromised product yield. To overcome this limitation, we have developed a specialized system for the creation of low-temperature lipases. In this study,

we isolated a high-yield strain capable of producing low-temperature lipase from soil samples gathered in cold forest regions, employing initial screening via the Rhodamine B method followed by re-screening with the p-nitrophenyl butyrate method. Subsequently, we generated a mutant strain exhibiting enhanced lipase activity and superior genetic stability through UV-nitrosoguanidine compound mutagenesis. Furthermore, we optimized the liquid fermentation conditions to augment lipase production. The lipase was purified using ammonium sulfate fractional precipitation, followed by anion exchange chromatography and gel filtration chromatography, and its lipaseology characteristics, including optimal temperature, pH, stability, and kinetics, were thoroughly evaluated. Compared with commercially available lipase, this lipase demonstrates a shorter reaction time, exerts minimal effect on substrate quality, and substantially mitigates the risk of thermal damage relative to conventional processes, thereby offering crucial technical support for the eco-friendly production of high-activity heat-sensitive products.

## Materials and Methods

### Materials and Reagents

Potato dextrose agar (PDA), peptone, beef extract, and sucrose were purchased from Haibo Biotech (Qingdao, China). Olive oil, rhodamine B, p-nitrophenol, Tris-HCl buffer, ammonium sulfate, p-Nitrophenyl palmitate, polyvinyl alcohol, magnesium sulfate, dimethyl carbonate, sodium hydroxide, and nitrosoguanidine were all sourced from Macklin Biochemical Technology Co., Ltd. (Shanghai, China). Bovine serum albumin, Coomassie Brilliant Blue G-250, lactose, and dextrin were purchased from Aladdin Biochemical Technology Co., Ltd. (Shanghai, China). HiTrap Q HP and Superdex 75 Increase 10/300 GL chromatography columns were obtained from

Cytiva (Massachusetts, United States). Organic solvents such as methanol, ethanol, acetone, acetonitrile, dimethyl sulfoxide, glycerol, ethyl acetate, and n-hexane were all purchased from Kemiou Chemical Reagent Co., Ltd. (Tianjin, China).

**Preparation of culture medium**

Enrichment medium: $(NH_4)_2SO_4$ 1.0 g, $K_2HPO_4$ 1.0 g, NaCl 0.5 g, $MgSO_4$ 0.1 g, yeast extract 2 g, emulsified olive oil solution 40 mL, distilled water 1000 mL, with a natural pH value, sterilize at 121℃ for 30 minutes.

Rhodamine B lipid-screening medium: $(NH_4)_2SO_4$ 1.0 g, $K_2HPO_4$ 1.0 g, KCl 0.5 g, $MgSO_4$ 0.2 g, $FeSO_4$ 0.01 g, agar powder 20 g, distilled water 1000 mL， with a natural pH value, sterilize at 121℃ for 30 minutes. After sterilization, cool the medium to approximately 60℃, then add 10 mL of a Rhodamine B solution (0.1 mg/mL) and 120 mL of emulsified olive oil. Both the emulsified olive oil and the Rhodamine B solution should be sterilized separately.

Potato Dextrose Agar (PDA) Take 46.0 grams of the PDA culture medium reagent and heat it to dissolve it in 1000 mL of distilled water. The pH value remains natural. Sterilize at 121℃ for 30 minutes.

Seed Culture Medium: Peptone 5 g, Sucrose 10 g, $K_2HPO_4$ 0.5 g, $MgSO_4$ 0.5 g, distilled water 1000 mL. For solid medium, add 20 g of agar powder. The pH value remains natural. Sterilize at 121℃ for 30 minutes.

Secondary Screening Fermentation Medium: Peptone 10 g, sucrose 3 g, $K_2HPO_4$ 2.0 g, $MgSO_4$ 0.5 g, 10 mL of emulsified olive oil, distilled water 1000 mL. The pH value remains natural. Sterilize at 121℃ for 30 minutes.

**Initial screening of lipase-producing microbial strains**

In the forest region of the Daxing'anling area in Heilongjiang Province (125°30′21″E, 51°20′05″N), the annual mean temperature ranges from -4℃ to -2℃, with an extreme minimum temperature reaching -52.3℃[19]. Soil samples were randomly collected from multiple locations within the 0-10 cm subsurface layer, following the removal of any animal or plant debris. Subsequently, 5 g of soil sample was weighed and added to 45 mL of 0.9% sterile physiological saline. The mixture was then placed in a constant-temperature shaker, shaken uniformly, and allowed to stand for 30 minutes. Thereafter, 2.5 mL of the supernatant was transferred to 100 mL of enrichment medium, and the culture was incubated at 20℃ with shaking at 160 r/min for 72 h. The enrichment culture was then subjected to gradient dilution with 0.9% physiological saline to obtain bacterial suspensions with concentrations ranging from $10^{-1}$ to $10^{-6}$. Aliquots of 100 μL from each dilution were spread onto Rhodamine B oil screening medium, with each treatment replicated three times. After incubation at 20℃ for 72 h, the plates were examined for colony growth. Colonies displaying distinct fluorescent halos under ultraviolet light were selected, diluted, and re-plated onto fresh Rhodamine B medium. These colonies were further incubated, and single colonies with pronounced fluorescent halos were isolated[20]. Finally, these isolated colonies were preserved in slant medium.

**Re-screening of lipase-producing Strains**

A loopful of the strain preserved in slant medium was inoculated into 30 mL of seed medium and incubated at 20℃ with shaking at 160 r/min for 48 hours. Subsequently, 2 mL of the seed culture was transferred into 30 mL of fermentation medium and incubated at 20℃ with shaking at 180 r/min for 72 h. Following liquid fermentation, the fermentation broth was centrifuged at 8000

r/min for 10 min at 4℃, and the supernatant was collected as the crude enzyme solution. The lipase activity of the crude enzyme solution was then measured[21].

**Determination of lipase activity**

Lipase activity was measured based on a slightly adjusted p-nitrophenol method[22]. Lipase was used to hydrolyze p-nitrophenol palmitate into colored p-nitrophenol, and then the absorbance value was measured with an ultraviolet spectrophotometer at 410 nm, and the lipase activity was calculated.

First, 20 mg lipase powder was dissolved in 400 μL Tris-HCl buffer, and the supernatant was centrifuged (8000 rpm, 10 min) as the lipase solution. Then, 20 μL of p-NPP (10 mmol/L) substrate solution was added to 780 μL of Tris-HCI buffer and preheated at 30℃ for 5 min, and then 200 μL of lipase solution was added. After 10 min of reaction, 1 mL of 0.5 mol/L trichloroacetic acid (0.5 mol/L) was added. After mixing, the reaction was terminated for 5 min, and 3 mL of 0.5 mol / L NaOH (0.5 mol/L) was added to adjust the pH value (200 μL of distilled water was replaced with 200 μL of lipase solution, and other conditions were unchanged, that is, blank). The absorbance was measured at 410 nm. The concentration of p-NP was calculated according to the standard curve, and then the lipase activity was calculated. Under certain conditions, the amount of lipase that released 1 μmol of p-NP per minute is defined as a lipase activity unit (U)[23]. The definition formula is as follows:

$$X=cV/tV'$$

where X is lipase activity (U/mL), c is the concentration of p-nitrophenol (μmol/L), v is the final volume of the reaction solution after acid-base adjustment (mL), v' is the amount of lipase solution (mL), and t is the action time (min).

The linear regression equation for the standard curve of p-NP is $y=0.0042x+0.0014$($R^2=0.9909$).

## Identification of lipase-producing strains

After activating the preserved strain, it was inoculated into PDA liquid medium. After 3 days, the liquid was aspirated and centrifuged at low temperature to obtain the cells of the strain in the logarithmic growth phase (weight > 300 mg). Fungal genomic DNA was extracted for PCR amplification. The PCR amplification used universal primers ITS1 (TCCGTAGGTGAACCTGCGG) and ITS4 (TCCTCCGCTTATTGATATGC). After electrophoresis separation of the PCR products, the target ITS fragment was recovered for sequencing[24]. The obtained sequence was compared with sequences of similar similarity using the BLAST tool in the GenBank database, and a phylogenetic tree was constructed using MEGA12.

## UV-Nitrosoguanidine mutagenesis breeding

### *Ultraviolet mutagenesis treatment.*

Take a slant culture medium preserved for the strain and activate it. Rinse it repeatedly with sterilized physiological saline and vigorously shake to disperse it into a spore suspension. Subsequently, adjust the concentration of the suspension to $10^6$ spores/mL using distilled water[25]. For UV mutagenesis, preheat the UV lamp for half an hour in advance to ensure light source stability and achieve sterilization, thereby preventing any potential effect on the experiment[26]. Add 10 mL of the single spore suspension to each plate, maintaining a distance of 350 mm between the petri dish and the light source, and set the wavelength to 245 nm. Expose the plates to UV radiation for varying durations: 0 s, 60 s, 75 s, 90 s, 105 s, 120 s, 135 s, 150 s, and 160 s, with the lid on, and conclude the exposure with the lid still on. Dilute the treated solution sequentially, and use a

pipette to transfer 100 μL onto PDA medium[25,27]. Conduct three parallel experiments for each group, with the non-UV-exposed group serving as the control. Incubate the plates upside down in a 20℃ incubator for 5 days, observe, and record the colony growth. Plot the UV mutagenesis lethal curve of *Aspergillus niger*, with UV exposure time on the x-axis and the mortality rate of the fungal cells on the y-axis, and calculate the lethal rate using formula 2

$$L(\%)=CFU_{initial}\text{-}CFU_{surviving}/CFU_{initial}\times 100\%$$

Where L is lethality rate (%), $CFU_{initial}$ is the initial viable count, $CFU_{surviving}$ is the viable count

***Mutagenic treatment with nitrosoguanidine.***

Dilute the spore suspension appropriately and spread it onto medium plates containing nitrosoguanidine at different concentration gradients (0.05%, 0.10%, 0.15%, 0.20%, 0.25%, 0.30%). Incubate the plates upside down in a 20℃ incubator for 5 days, observe, and record the colony growth. Plot the lethal curve of *Aspergillus niger* induced by nitrosoguanidine[28], with the concentration of nitrosoguanidine on the x-axis and the mortality rate of the fungal cells on the y-axis.

***UV-Nitrosoguanidine Combined Mutagenesis Treatment.***

After subjecting the spore suspension to the optimal UV mutagenesis conditions, evenly spread it onto a plate containing rhodamine B-coated oil under the optimal nitrosoguanidine mutagenesis conditions. Incubate the plate upside down in a 20℃ incubator for 5 days, followed by observation and recording.

***Selection of Mutant Strains.***

(1) Preliminary Screening

Select strains exhibiting larger fluorescent circles following UV-Nitrosoguanidine mutagenesis. Record and compare the ratio (D/d) of the fluorescent circle diameter (D) to the colony diameter (d) with that of the original strain. Mutant strains with a higher D/d ratio than the original strain should be chosen for subculturing, numbering, and preservation[29,30].

(2) Re-screening

Inoculate a loopful of the mutant strain obtained from preliminary screening into the seed medium to prepare the seed solution. Add this seed solution to the fermentation medium and incubate at 20℃ with shaking at 80 r/min for 72 h. After liquid fermentation, centrifuge the fermentation broth at 8000 r/min for 10 min at 4℃, and collect the supernatant as the crude enzyme solution for lipase activity measurement.

***Genetic Stability Experiment of Mutant Strains.***

Following re-screening and breeding, the high-yield lipase-producing strain was continuously cultured for five generations[31]. Each generation was inoculated into a fermentation medium for fermentation, and the lipase activity produced was measured to assess the genetic stability of the mutant strain.

**Optimization of Enzyme Production Conditions in Liquid Fermentation**

***Effect of Temperature on Lipase Production Activity.***

Adjust the fermentation temperature to 10, 15, 20, 25, 30, 35, and 40℃, respectively[13]. Inoculate with $2\times10^6$ spores, maintain a shaking speed of 160 r/min, and incubate on a shaker for 72 h.

Measure the lipase activity at each temperature to identify the optimal temperature for lipase production during fermentation.

***Effect of pH on Lipase Production Activity.***

Adjust the pH of the fermentation medium to 5.0, 6.0, 7.0, 8.0, and 9.0, respectively. Inoculate with $2\times10^6$ spores and incubate at 20℃ with shaking at 160 r/min for 72 hours. Measure the lipase activity at each pH level to determine the optimal pH for enzyme production during fermentation.

***Influence of Inoculum Size on Lipase Production Activity.***

Adjust the concentration of the spore suspension and inoculate the fermentation medium with varying inoculum sizes of $2\times10^6$, $4\times10^6$, $6\times10^6$, $8\times10^6$, and $1\times10^7$ spores[32]. Incubate at 20℃ with shaking at 160 r/min for 72 h and measure the lipase activity separately to ascertain the optimal inoculum size for fermentation enzyme production.

***Effect of Nitrogen Sources on Lipase Production Activity.***

Maintain the other components of the fermentation medium constant while adjusting the nitrogen sources to beef extract, peptone, ammonium sulfate, sodium nitrate, and potassium nitrate, each at a concentration of 10 g/L. Inoculate with $2\times10^6$ spores and add to fermentation media containing different nitrogen sources. Incubate at 20℃ with shaking at 160 r/min for 72 h and measure the lipase activity separately to identify the optimal nitrogen source for fermentation.

***Effect of Carbon Sources on Lipase Production Activity.***

Keep the other components of the fermentation medium unchanged while adjusting the carbon sources to glucose, sucrose, lactose, and dextrin, each at a concentration of 3 g/L. Inoculate with $2\times10^6$ spores and add to fermentation media containing different carbon sources. Incubate at 20℃ with shaking at 160 r/min for 72 h and measure the lipase activity to determine the optimal carbon source for fermentation.

***Analysis of Optimization Results Using Response Surface Methodology.***

The response surface experiment primarily addresses multiple factors and determines their significant effects on the response variable. Based on the results of the single-factor experiment, the Box-Behnken experimental design was employed to investigate three factors: A: temperature (℃), B: pH, and C: inoculum size (spores). Lipase activity (U/mL) serves as the response value for the three-factor, three-level response surface, as shown in Table 1.

## Separation and Purification of Lipase

***Preparation of Crude Lipase Solution***

Activate a preserved strain of *Aspergillus niger* Y-B04, then inoculate it into a liquid fermentation medium. Incubate at 20℃ on a shaker for 72 h, followed by filtration of the fermentation broth using a 0.45 μm filter membrane. Collect the filtrate to remove insoluble impurities. Transfer the filtrate into a centrifuge tube, centrifuge at 8000 r/min for 10 min at 4℃, and collect the supernatant as the crude lipase enzyme solution.

***Determination of Protein Content Using the Coomassie Brilliant Blue Method***

In this study, the Coomassie Brilliant Blue method was employed to quantify protein content. Coomassie Brilliant Blue G-250, a dye that binds to proteins, produces a cyan color upon binding and exhibits maximum absorbance at 595 nm[33]. The reaction between Coomassie Brilliant Blue G-250 and proteins reaches equilibrium within 2 min, indicating a rapid response. Moreover, the resulting complex remains stable for over 30 min at room temperature. This method offers advantages such as simple and safe reagents, ease of operation, and a sensitivity four times higher than that of the Lowry method. Therefore, the Coomassie Brilliant Blue method was selected for protein content determination in this study[34].

The linear regression equation for the protein standard curve is $y = 0.0073x + 0.423$($R^2$=0.9981).

***Determination of the Salting-Out Range of Ammonium Sulfate***

Take a sample of crude lipase enzyme solution and distribute equal volumes into 10 conical flasks. Place the flasks on a magnetic stirrer and gradually add ammonium sulfate to each flask until saturation levels of 10%, 20%, 30%, 40%, 50%, 60%, 70%, 80%, 90%, and 100% are reached, respectively. After complete dissolution and stirring, refrigerate the solutions at 4℃ overnight to facilitate precipitation. The following day, centrifuge the solutions at 10000 r/min for 15 min at 4℃[35]. Measure the lipase activity in the supernatant, then redissolve the precipitate in an equal volume of distilled water and measure the lipase activity again[36]. Record the results and plot the ammonium sulfate fractional precipitation curve.

***Salting-Out with Ammonium Sulfate***

Transfer the crude lipase enzyme solution into a beaker and place it on a magnetic stirrer. Gradually and uniformly add finely ground ammonium sulfate while stirring until a saturation of

30% is achieved. Refrigerate overnight at 4℃. The next day, centrifuge at 10000 r/min for 15 min at 4℃. Collect the supernatant and repeat the process of adding ammonium sulfate, this time to a saturation of 60%. Refrigerate overnight at 4℃ again. On the following day, centrifuge at 10,000 r/min for 15 min at 4℃, discard the supernatant, and retain the precipitate as the purified lipase.

***Dialysis Desalination***

Dissolve the lipase obtained from ammonium sulfate salting-out in Tris-HCl buffer solution. Transfer the lipase solution into a dialysis bag (MW 8000-14000 Da) and desalt it by refrigerating at 4℃. Use deionized water as the dialysis solution. Consider desalting complete when no precipitate forms after adding $BaCl_2$ to the filtrate[35]. Freeze-dry the desalted lipase and store it in the refrigerator for future use.

***Anion Exchange Chromatography***

Reconstitute the lyophilized enzyme powder using Tris-HCl buffer (20 mmol/L, pH 7.5) and subject it to Q-HP strong anion exchange chromatography[37]. Use Tris-HCl buffer (20 mmol/L, pH 7.5) as loading buffer A and NaCl solution (1.0 mol/L) as eluent B. Set the flow rate at 2 mL/min with the following gradient: 100% A, 0% B for 15 bed volumes (BV); 90% A, 10% B for 15 BV; 80% A, 20% B for 15 BV. Collect the effluent, measure the absorbance at 280 nm, and calculate the lipase activity and protein content[37].

***Gel Filtration Chromatography***

Perform the experiment using a Superdex 75 gel filtration chromatography column with a flow rate of 1 mL/min. Elute with Tris-HCl buffer (20 mmol/L, pH 7.5), collect the effluent, measure the absorbance at 280 nm, and calculate the lipase activity and protein content[38].

**Enzymatic Properties of Lipase**

***Determination of the Optimal Reaction Temperature for Lipase***

Set the reaction temperatures to 15℃, 20℃, 25℃, 30℃, 35℃, 40℃, 45℃, and 50℃ while maintaining other conditions constant. Measure the lipase activity at each temperature. Conduct three parallel experiments at each temperature, record the results, and determine the optimal reaction temperature for lipase.

***Determination of the Optimal Reaction pH for Lipase***

Adjust the reaction pH to 4.0, 5.0, 6.0, 7.0, 8.0, 9.0, and 10.0 using phosphate buffer, Tris-HCl buffer, and sodium carbonate buffer, respectively, while keeping other conditions constant. Measure the lipase activity at each pH. Conduct three parallel experiments at each pH, record the results, and determine the optimal reaction pH for lipase.

***Determination of Temperature Stability of Lipase***

Dissolve the lipase powder in Tris-HCl buffer solution and incubate the lipase solution in a water bath at 4℃, 20℃, 30℃, 40℃, 50℃, and 60℃ for 6 h. Take samples of the lipase solution for cooling every hour during incubation. Measure the lipase activity using the p-nitrophenyl method.

Conduct three parallel experiments at each temperature to evaluate the temperature stability of lipase.

***Determination of pH Tolerance of Lipase***

Dissolve the lipase powder in citric acid-sodium citrate buffer (pH 5.0), phosphate buffer (pH 6.0), Tris-HCl buffer (pH 7.0-8.0), and sodium carbonate-sodium bicarbonate buffer (pH 9.0-10.0), respectively. Incubate at 4℃ for 1-5 h, adjust the pH back to the optimal reaction pH, and measure the lipase activity using the p-nitrophenyl method. Conduct three parallel experiments at each pH, record the results, and assess the pH tolerance of lipase.

***Influence of Metal Ions on Lipase***

Prepare Tris-HCl buffer solutions containing $Na^{+}$, $Mg^{2+}$, $Ca^{2+}$, $Fe^{3+}$, $Mn^{2+}$, $K^{+}$, $Zn^{2+}$, and $Cu^{2+}$ at concentrations of 1 mM/L and 10 mM/L, respectively[39]. Incubate at 30℃ for 1 h and measure the residual lipase activity. Calculate the results using the activity in the absence of metal ions as a control.

***Effect of Organic Solvents on Lipase***

Dissolve the lipase powder in Tris-HCl buffer and add organic solvents (methanol, ethanol, acetone, acetonitrile, dimethyl sulfoxide, glycerol, ethyl acetate, n-hexane) to achieve concentrations of 10% and 20% (v/v)[39]. Store at 30℃ with shaking at 200 rpm for 24 h and measure the residual lipase activity. Use the activity in the absence of organic solvents as a control for calculation.

### *Substrate Specificity of Lipase*

According to the lipase activity assay method described in Section 2.5, measure the lipase activity using p-nitrophenyl esters (p-NPC2, p-NPC4, p-NPC6, p-NPC8, p-NPC10, p-NPC12, p-NPC14, p-NPC16, p-NPC18) with varying carbon chain lengths as substrates. Calculate the lipase activity relative to the substrate with the highest lipase activity, set as 100%.

### *Kinetic Determination of Enzymatic Reaction*

Prepare p-NPP solutions at concentrations of 1, 2, 3, 4, 5, 6, 7 and 8 mM, measure their reaction rates, and plot the Lineweaver-Burk double reciprocal plot of 1/S versus 1/V. Determine the Michaelis constant (Km) and maximum reaction rate (Vm) of the protease from the plot[40], where the horizontal intercept represents -1/Km and the vertical intercept represents 1/Vm.

### Statistical analysis

Statistical analysis was performed using SPSS 19.0 software with one-way ANOVA and a significance level set at $p < 0.05$. Data were expressed as mean ± standard deviation. All experiments were conducted at least in triplicate.The combination of response surface methodology conditions was optimized using Design-Expert 13.0 software, enabling comprehensive residual analysis and model fitting assessment.

## Results

### Screening of strains producing low-temperature lipase

In the experiment, soil samples were collected from low-temperature forest regions, and a total of 54 bacterial strains were isolated and purified following enrichment culture. After initial screening using a rhodamine B-based medium, lipase-producing strains hydrolyzed olive oil into free fatty acids, which subsequently bound specifically to rhodamine B, resulting in the formation of orange fluorescent halos under ultraviolet illumination. A larger fluorescent halo indicated higher lipase activity. Ultimately, three strains exhibiting larger fluorescent halos were identified, as depicted in Figure 1(a), suggesting their robust lipase-producing capabilities. These strains were designated as Y-A01, Y-A02, and Y-A03, with strain Y-A02 displaying the largest fluorescent halo. Subsequently, the lipase activities of the crude enzyme extracts from these three strains were compared through re-screening, leading to the identification of the strain with the highest lipase-producing capacity.

Following shake flask fermentation of the three initially screened strains, all demonstrated favorable lipase activity, as illustrated in Figure 1(b). Notably, strain Y-A02 exhibited the highest lipase activity, measuring 21.50±1.54 U/mL. This activity surpassed that of *Bacillus cereus I13*, which was isolated by Hafsa K[41] et al. from Arctic sediments and demonstrated a low-temperature lipase activity of 11.42 U/mL. Furthermore, compared to *Lactococcus lactis grx602*, isolated by Yu P[42] et al. from dairy products with a lipase activity of 12.43 U/mL, strain Y-A02 also displayed a significantly higher lipase activity. This superior performance may be attributed to the inherent characteristics of fungi, including vigorous growth, relatively straightforward fermentation conditions, and robust extracellular lipase secretion capabilities[32].

**Identification results of lipase-producing strain Y-A02**

Genomic DNA was extracted from the strain, followed by PCR amplification and subsequent detection of the ITS region sequence. The molecular weight of the DNA fragment from strain Y-A02, as determined by SDS-PAGE electrophoresis, is depicted in Figure 2(a), revealing a DNA fragment size of 562 bp. The sequenced result was aligned in NCBI, and the sequence with the highest similarity was chosen for species identification. Ultimately, it was confirmed that strain Y-A02 exhibits 99% homology with the *Aspergillus niger* genus. Based on the alignment results, a phylogenetic tree was constructed using the Maximum Likelihood method[11,43], as illustrated in Figure 2(b), indicating the closest genetic relationship with strain KF691796.1 *Aspergilus niger* isolate EFB1. By integrating the biochemical identification results of strain Y-A02 with the phylogenetic tree analysis, it was concluded that Y-A02 is indeed *Aspergillus niger*.

## Results of Y-A02 Mutagenesis Treatment

### *Results of UV Mutagenesis Treatment.*

Ultraviolet (UV) light has the capacity to damage DNA structure, triggering base mutations or strand breaks, and is thus extensively employed as a physical mutagen in microbial breeding[44] . Moderate DNA damage can activate the error-prone repair mechanisms in fungi, offering a viable approach for the targeted enhancement of extracellular enzyme secretion. *Aspergillus niger* Y-A02 was subjected to UV irradiation for varying durations to determine the lethality rates at different time points. The UV mutagenesis lethality curve is presented in Figure 3(a). As the duration of UV irradiation increases, the lethality rate of *Aspergillus niger* also rises significantly. In mutagenesis breeding, a lethality rate of 75-85% is typically chosen to enhance the likelihood of

positive mutations[45]. At a UV irradiation time of 120 s, the lethality rate reaches 82.9%. Consequently, this study selected 120 s as the optimal mutagenesis duration. Consequently, this study selected 120 s as the optimal mutagenesis duration.

***Results of Nitrosoguanidine Mutagenesis Treatment***

Nitrosoguanidine (NTG), recognized as a highly effective chemical mutagen, specifically alkylates DNA bases, inducing a significantly higher frequency of point mutations compared to UV mutagenesis. Its mutagenic mechanism is more precise, and the mutation spectrum is more focused[46]. *Aspergillus niger* Y-A02 was used as the starting strain and cultured on media containing varying concentrations of NTG to determine the lethality rates. The NTG-induced lethality curve is shown in Figure 3 (b). As the NTG concentration increases, the lethality rate of *Aspergillus niger* also rises markedly. At an NTG concentration of 0.15%, the lethality rate reaches 78.9%. Therefore, NTG mutagenesis was selected for this experiment, with a treatment concentration of 0.15%.

***Results of UV-Nitrosoguanidine Combined Mutagenesis Treatment***

Compound mutagenesis, leveraging the synergistic effects of UV radiation and NTG, results in complementary and overlapping DNA damage, significantly enhancing the mutation rate and diversity[47]. Following a 120s UV pretreatment, the strains were treated with 0.15% NTG. Strains with larger fluorescent halos were selected for shake flask fermentation, and their lipase production was measured, recorded, and compared. The comparison of fluorescent halos is shown in Figure 4, and the results of lipase production before and after compound mutagenesis are presented in Table 2.

As indicated in Table 2, 15 *Aspergillus niger* strains with notably larger fluorescent halos after UV-NTG compound mutagenesis were selected to determine the ratio of fluorescent halo diameter to colony diameter (D/d) and lipase activity. According to the experimental results, as the D/d value increases, the lipase activity generally increases. Among them, the mutant strain Y-B04, with a D/d value of 1.86 after UV-NTG compound mutagenesis, exhibited the highest lipase activity, reaching 48.88±1.94 U/mL, which represents a 127.35% increase compared to the initial strain [(21.50±1.54) U/mL]. This significant improvement underscores the efficiency and synergistic effect of UV-NTG compound mutagenesis in directionally enhancing lipase secretion.

***Genetic Stability Results of Mutant Strains.***

To assess the genetic stability of the mutant strains, five *Aspergillus niger* mutant strains with high lipase activity—Y-B02, Y-B04, Y-B11, Y-B14, and Y-B15—selected from the UV-NTG compound mutagenesis results, were continuously subcultured for five generations. The lipase activity produced by each strain was measured to evaluate genetic stability, with the results shown in Table 3.

The lipase activity of strain Y-B04 remained within the range of 48.45–50.21 U/mL across five generations, with a fluctuation of only ±1.76 U/mL, demonstrating significantly better stability than the other strains. In contrast, the activity of Y-B14 gradually decreased with each generation, with a 12.07% reduction in the fifth generation compared to the initial generation, indicating a propensity for loss of mutant traits. Overall, Y-B04 exhibits excellent genetic stability and potential for industrial application.

**Optimization of lipase production through liquid fermentation**

According to Figure 5(a), lipase activity peaks at 20℃, reaching 56.49±2.32 U/mL, representing the optimal condition for liquid fermentation of lipase by *Aspergillus niger* Y-B04. At 20℃, *Aspergillus niger* exhibits optimal growth, facilitating better growth and full release of lipase. When the temperature is too low, the growth rate of *Aspergillus niger* slows, prolonging fermentation time and delaying lipase release; conversely, when the temperature exceeds 30℃, the enzyme protein conformation becomes unstable, and the spatial structure of the active site undergoes irreversible distortion[48], resulting in a sharp 41.49% decrease in activity.

According to Figure 5(b), lipase activity reaches a maximum of 60.88±2.13 U/mL at a pH of 6.0, which is 20.14% and 11.63% higher than at pH 5.0 and 7.0, respectively. At pH levels below 5.0, cellular metabolism is inhibited, reducing extracellular protein secretion. At pH levels above 7.0, the surface charge distribution of enzyme molecules becomes imbalanced, disrupting the hydrogen bonding network and significantly decreasing catalytic efficiency[49,50]. A pH of 6.0 aligns with the optimal microenvironment for extracellular lipase in *Aspergillus niger*, balancing cellular activity and enzyme stability.

According to Figure 5(c), when the inoculum size is $6\times10^6$ spores, enzyme activity reaches 55.48±1.56 U/mL. An inoculum size that is too low delays entry into the logarithmic phase, prolonging the fermentation period and delaying enzyme production; conversely, an inoculum size that is too high limits dissolved oxygen, accumulates metabolic by-products, and inhibits enzyme synthesis. At this inoculum size, cellular density and metabolic load achieve an optimal balance[51], with high spore activity and good synchronicity within a unit volume, maximizing lipase synthesis efficiency.

According to Figure 5(d), organic nitrogen sources significantly outperform inorganic nitrogen sources, with peptone being the optimal choice, yielding an enzyme activity of 55.67±2.13 U/mL. Organic nitrogen sources are rich in proteins, free amino acids, and growth factors that can be directly absorbed and utilized by cells, promoting rapid cell proliferation and efficient expression of lipase genes. In contrast, inorganic nitrogen sources provide a single nutrient that requires complex metabolic transformation, resulting in high energy consumption and slow rates, leading to delayed enzyme synthesis initiation and lower peak values[52]. Additionally, the metabolic process of inorganic nitrogen sources significantly alters environmental pH, and drastic pH fluctuations may inhibit microbial growth or even cause cell death, whereas the metabolic products of organic nitrogen sources have a minimal effect on pH.

According to Figure 5(e), carbon sources significantly influence lipase activity, with sucrose being the optimal choice, achieving an enzyme activity of 57.32±2.02 U/mL. *Aspergillus niger* secretes invertase to hydrolyze sucrose into glucose and fructose, which are directly and efficiently utilized by the fungus, meeting the energy requirements for rapid growth and avoiding the carbon catabolite repression effect caused by single glucose. However, due to the lack of β-galactosidase in *Aspergillus niger*, lactose utilization is limited[53]. Dextrin is gradually degraded into glucose by amylase, but insufficient amylase activity results in slow dextrin utilization, failing to provide timely energy and precursors.

**Response surface optimization experiment results**

Based on the single-factor experiment, three factors were selected: A temperature (℃), pH value, and inoculum size (spores). Experiments were designed according to Table 1, and response surface analysis was performed using Design-Expert 12.0 software for optimization. The experimental results of optimizing the conditions for lipase production by *Aspergillus niger* fermentation are shown in Table 4

***Model Development and Statistical Evaluation***

Quadratic response surface regression modeling was performed on the experimental data presented in Table 4 using Design-Expert 12.0 software. The resulting second-order polynomial model describing lipase activity (Y) as a function of temperature (A, ℃), pH (B), and inoculum concentration (C) is given by:

$$Y=57.70+1.45A-0.2925B+2.28C-0.6475AB+1.09AC+0.1025BC-4.87A^2-3.78B^2-6.22C^2$$

The test results of the regression model coefficients are shown in table 5.

The larger F-statistic and smaller p-value in the analysis of variance (ANOVA) of the regression model indicate greater statistical significance of the corresponding terms. As presented in Table 5, the model's overall p-value was $< 0.0001$, confirming that the quadratic response surface regression model is highly statistically significant and exhibits an excellent fit to the experimental data. The p-value for the lack-of-fit test was 0.1329 ($> 0.05$), indicating that the lack of fit was nonsignificant—thus supporting the adequacy and reliability of the model. Additional model diagnostics further corroborate its robustness: the coefficient of variation (CV) was 1.23%, reflecting high experimental precision and reproducibility; the adjusted $R^2$ (0.9862) and predicted $R^2$ (0.9538) demonstrate strong explanatory power and predictive capability; the Pearson correlation coefficient between

observed and predicted responses was 0.9940, indicating an exceptional degree of linear association; and the signal-to-noise ratio (29.0231) far exceeds the threshold of 4, confirming the model's suitability for reliable experimental optimization and practical application. Collectively, these metrics validate the appropriateness of the response surface methodology for optimizing lipase production by *Aspergillus niger*, with respect to the three critical variables—temperature, pH, and inoculum volume.

According to the ANOVA results, the linear effects of factor A (temperature) and factor C (inoculum volume) on the response (lipase activity, Y) were highly significant ($p < 0.001$), whereas factor B (pH) exhibited no statistically significant linear effect ($p > 0.05$). Among the two-factor interaction terms, only the AC interaction was statistically significant ($p < 0.05$), while AB and BC interactions were nonsignificant ($p>0.05$). All quadratic terms ($A^2$, $B^2$, and $C^2$) were highly significant ($p < 0.001$), suggesting pronounced curvature in the response surface with respect to each variable. Based on comparative magnitudes of the F-statistics, the relative influence of the three factors on lipase activity follows the order: inoculum volume > temperature > pH.

Response Surface Analysis. To further elucidate the nature and strength of factor interactions, three-dimensional (3D) response surface plots and corresponding contour plots were generated based on the fitted regression model (Figures 6-8).

In such visualizations, a steep 3D surface coupled with elliptical contour lines indicates a strong interactive effect between the two variables; conversely, a relatively flat surface and near-circular contours suggest weak or negligible interaction. As shown in Figures 6-8, the AC interaction displays marked curvature—evidenced by a steep 3D surface and distinctly elliptical contours—consistent with its statistically significant ANOVA result.

In contrast, the AB and BC interactions yield nearly circular contours and gently sloping surfaces, corroborating their nonsignificance in the ANOVA. Notably, the conclusion regarding AC as the sole significant interaction term is thus reinforced both quantitatively (via ANOVA) and qualitatively (via graphical interpretation).

### *Experimental Validation of the Optimized Conditions*

Using Design-Expert® 12.0 software, the global optimum for lipase production by *Aspergillus niger* was predicted as follows: temperature = 20.87°C, pH = 5.95, and inoculum volume = $6.40\times10^6$ spores/mL, yielding a predicted lipase activity of 58.06 U/mL. To verify model accuracy and operational feasibility under realistic fermentation conditions, three independent validation experiments were conducted at practically rounded settings: 21°C, pH 6.0, and inoculum volume of $6.5\times10^6$ spores/mL. The experimentally measured mean lipase activity was 57.26±0.41 U/mL, representing a deviation of only 1.4% from the model prediction. This close agreement confirms the validity, predictive accuracy, and practical utility of the developed response surface model for optimizing lipase fermentation by *Aspergillus niger*.

## Isolation and Purification of Lipase

Extracellular lipase was isolated from the fermentation supernatant through a sequential purification strategy comprising ammonium sulfate precipitation, dialysis, anion-exchange chromatography (DEAE-Sepharose FF), and size-exclusion chromatography (Superdex 75). Initial analysis revealed that the crude enzyme preparation contained substantial amounts of contaminating proteins. Ammonium sulfate

precipitation was employed to selectively enrich lipase while removing non-target proteins; optimization studies (Figure. 9a) indicated that precipitation at 30% saturation effectively removed highly abundant impurities—evidenced by high precipitate yield but low specific activity—whereas precipitation at ≥60% saturation yielded significantly higher specific activity in the pellet, with diminishing returns beyond this threshold[54]. This suggested near-complete lipase aggregation and recovery at 60% saturation. Accordingly, a two-step ammonium sulfate fractionation was adopted: first at 30% saturation to remove bulk contaminants, followed by precipitation at 60% saturation to recover lipase.

The resulting precipitate was desalted by dialysis and subsequently loaded onto a DEAE-Sepharose FF column. Elution yielded three distinct protein peaks (Figure. 9b). Peak 1 corresponded to non-anionic or weakly anionic proteins eluting in the flow-through/wash fraction; Peak 2 represented proteins exhibiting moderate affinity for the anion-exchange matrix; and Peak 3 comprised strongly bound, highly anionic proteins requiring elevated ionic strength for elution. Enzymatic assays across fractions identified Peak 2 as containing the highest lipase-specific activity; therefore, the fraction exhibiting maximal activity within this peak was pooled for further processing[55]. Subsequent size-exclusion chromatography on Superdex 75 (Figure. 9c) achieved final homogeneity, yielding electrophoretically pure lipase, as confirmed by SDS-PAGE, which displayed a single band of approximately 36 kDa (Figure. 9d).

Purification performance is summarized in Table 6. Following the three-stage protocol, lipase specific activity increased from 8.02 U/mg protein in the crude extract to 113.52 U/mg in the final preparation—a 14.15-fold purification. The overall activity recovery

was 1.79%. The consistent removal of contaminating proteins and preservation of enzymatic activity across all steps demonstrate the robustness and reproducibility of this protocol, supporting its applicability for scalable production of *Aspergillus niger* lipase.

## Enzymatic properties of lipase

### *Effect of temperature on lipase activity*

Temperature exerts a profound influence on lipase activity. As illustrated in Figure 10(a), the enzyme exhibits maximal activity at 30 ℃, and retains over 80% of its relative activity within the temperature range of 20–40 ℃. This pronounced catalytic efficiency under relatively low-temperature conditions aligns with the defining characteristics of a cold-adapted lipase. Further assessment of thermal stability revealed that the enzyme retained more than 80% of its initial activity after incubation at 4 ℃ or 20 ℃ for 5 h (Figure 10(b)). In contrast, activity declined markedly upon exposure to temperatures above 30 ℃; notably, after 1 h at 50 ℃, residual activity dropped to less than 20% of the initial value. This irreversible thermal inactivation arises from high-temperature-induced structural perturbations—including disruption of the enzyme's precise three-dimensional conformation, distortion of the active-site architecture, weakening of hydrophobic interactions, and acceleration of autolytic degradation[48]. Cold-adapted lipases typically exhibit reduced thermostability, a feature intrinsically linked to their evolutionary adaptation to low-temperature environments, where enhanced molecular flexibility of polypeptide segments is essential to sustain catalytic competence[49].

### *Effect of pH on lipase activity*

As shown in Figure 10(c), the lipase exhibited optimal activity at pH 7.0, retaining over 80% of its relative activity within the pH range of 6.0–7.0. Outside this range, enzymatic activity declined sharply-a phenomenon closely associated with alterations in the protonation states of key amino acid residues located in the active site[56]. At elevated pH values, deprotonation of residues such as tyrosine or lysine occurs, disrupting catalytic functionality. Moreover, pH-induced changes perturb the overall charge distribution across the enzyme molecule, thereby compromising critical structural elements—including salt bridges and hydrogen-bonding networks—that stabilize the tertiary structure[57]. Consequently, the microenvironment surrounding the catalytic center is destabilized, leading to diminished enzymatic performance.

***Effect of metal ions on lipase activity***

As shown in figure. 10(d), at a concentration of 1 mM, $Ca^{2+}$, $Na^{+}$, and $K^{+}$ each induced significant activation of lipase, increasing its relative activity to 104.12%, 47.52%, and 31.43%, respectively. This activation is likely attributable to the formation of ternary complexes between these metal ions and lipase, which stabilize the lipase's catalytically active conformation. Moreover, interactions between the metal ions and both the lipase and substrate may induce favorable conformational changes-enhancing molecular recognition, substrate binding, and subsequent catalysis and thereby augment lipase activity.

However, when the concentrations of $Ca^{2+}$ and $K^{+}$ were increased to 10 mM, their activating effects on lipase were retained, albeit at reduced magnitudes. In contrast, at $Na^{+}$ concentrations exceeding that of $Ca^{2+}$, the relative activity of lipase declined to 62.94%.

This attenuation may arise from competitive occupation of positively charged sites on the lipase surface by excess $Na^+$ ions. Furthermore, elevated ionic strength may compress the interfacial electric double layer, thereby weakening electrostatic interactions between the lipase and the interface and ultimately suppressing interfacial activation of the lipase[58]. $Mg^{2+}$, $Fe^{3+}$, $Mn^{2+}$, $Zn^{2+}$, and $Cu^{2+}$ significantly inhibited lipase activity at concentrations of 1 mM and 10 mM. Except for $Mg^{2+}$, these ions are all heavy metal ions, which can bind to key groups such as sulfhydryl and amino groups in the lipase molecule. This binding alters the charge distribution and spatial structure of the lipase molecule, thereby influencing the lipase activity[59]. The inhibition of lipase by heavy metal ions is frequently irreversible. $Mg^{2+}$ is distinctive in that, in most reports, it has minimal effect on lipase activity. The notable inhibitory effect on lipase in this study may be attributed to the high rigidity of the low - temperature lipase itself. The small radius and high charge density of $Mg^{2+}$ enable it to readily form strong coordination bonds with negatively charged carboxyl or phosphate groups in the lipase molecule[60]. This leads to a further increase in local conformational rigidity, weakens the flexibility of the active center, and consequently inhibits the catalytic efficiency.

***Effect of organic solvents on lipase activity***

As depicted in Figure 10(e), the majority of organic solvents exhibit an inhibitory effect on lipase activity at concentrations of 10% and 20%. This is primarily due to their ability to disrupt the native conformation of the lipase, cause the breakage of hydrogen bonds and ionic bonds, and also impact the diffusion of substrates and products. Organic solvents with high polarity can deprive the lipase of essential water, leading to the

inactivation of lipase molecules. A higher polarity may exert a more pronounced influence on lipase. Nevertheless, methanol at a concentration of 10% had a positive effect on lipase, enhancing its activity by 18.41%. This might be attributed to the fact that the solvent moderately enhanced interfacial mobility at low concentrations. The lipase achieved interfacial activation at the oil - water interface through the opening of the "lid" structure, and maintained a sufficient interfacial area to continuously expose the active center of the lipase molecules and sustain high catalytic efficiency[61].

***Substrate specificity exploration***

As presented in Table 7, the low-temperature lipase exhibited distinct hydrolysis activities towards substrates with varying chain lengths. Among these, the relative activity towards medium- and long-chain fatty acid (C8 - C12) substrates was relatively higher. Short-chain substrates might be unable to effectively induce the conformational change of the "cap" structure and are challenging to be recognized and hydrolyzed by the lipase. In contrast, long-chain substrates are prone to non-specific adsorption on the lipase surface due to their strong hydrophobicity. Consequently, the active center is obscured, or substrate diffusion is impeded, leading to a reduction in catalytic efficiency[62]. Therefore, substrate C8 demonstrated the highest relative activity (100%), followed by C10 (77.04%) and C12 (62.07%), while C2 - C6 and C14 - C18 showed relative activities lower than 60%. This substrate specificity is well - adapted to the natural physiological function of cryolipases, which is to efficiently hydrolyze medium- and long-chain lipids to fulfill the energy metabolism requirements of microorganisms at low temperatures.

***Determination of kinetic parameters of enzymatic reaction***

The Lineweaver-Burk double reciprocal plot drawn according to 1/[S]-1/V is shown in Figure 11, and the Mie constant Km=19.86mmol/L and the maximum reaction rate Vm=0.178mmol/(L·min) are calculated. The Km value indicates that the enzyme has a medium affinity for the substrate, which is slightly higher than that of most mesophilic lipases (usually 2-10 mmol/L), but it still maintains a high catalytic efficiency at low temperature. Although the binding of its active center to the substrate is not tight, it is more conducive to the rapid dissociation and turnover of the substrate at low temperature. Vm reflects the upper limit of the substrate that a single enzyme can convert per unit time, which is sufficient to efficiently drive lipid metabolism in a low temperature environment.

## Discussion

In this research, we concentrated on the screening and optimization of low - temperature lipase - producing *Aspergillus niger* from low - temperature extreme environments. We successfully acquired a high - temperature lipase - producing *Aspergillus niger* and systematically optimized its fermentation conditions. The findings indicated that under the optimized fermentation conditions, the production of low - temperature lipase was notably enhanced, and the lipase exhibited high catalytic activity at low temperatures. The core significance of this outcome lies in the fact that it not only offers an efficient and stable microbial source for low - temperature lipase production but also reveals the molecular mechanism through which this strain efficiently expresses lipase under low - temperature conditions, presenting a novel perspective for comprehending microbial adaptation strategies in extreme environments.

In terms of scientific connotation, the efficient expression of low - temperature lipase is closely associated with the genetic background, metabolic regulatory network, and environmental

adaptability of the strain. In this study, mutagenesis breeding and optimization of fermentation conditions might have activated key genes related to lipase synthesis in the strain and augmented the flux of its metabolic pathways, leading to improved enzyme production. Simultaneously, the low - temperature environment may induce a series of molecular changes to adapt to low temperatures, such as the adjustment of cell membrane fluidity and the increase in the flexibility of the lipase molecular structure, which jointly promote the efficient catalysis of cryogenic lipase at low temperatures.

Compared with other published studies, our research demonstrated consistency in several aspects, yet there were also significant disparities. In terms of consistency, this study and other studies have reported strategies for screening microorganisms from extreme environments to obtain enzymes with specific properties, suggesting that extreme environments are crucial resources for mining new biocatalysts. Additionally, similar methods were employed in this study to enhance lipase production, such as mutation breeding, optimization of fermentation conditions, and lipase isolation and purification, which have been extensively verified to be effective in improving lipase production. However, the differences were equally prominent. On the one hand, the catalytic activity of the cryo - lipase obtained in this study was higher than that of many similar lipases reported at low temperatures, which may be attributed to the unique genetic background and metabolic properties of the strains screened in this study. On the other hand, a more substantial increase in lipase production was achieved in this study, which may be due to the mutation breeding strategy and more refined fermentation and purification control adopted in this study.

We are fully cognizant that there are certain limitations to this study. For instance, the strains obtained in this study demonstrated good stability under laboratory conditions, but the

performance of the strains may be influenced by numerous factors during the industrial production process. Therefore, it is necessary to further explore methods for strain preservation and rejuvenation. Secondly, the potential for industrial application requires further evaluation. Although this study achieved remarkable results under laboratory conditions, to translate these results into industrial production, a comprehensive assessment of production cost, process feasibility, product safety, etc., is required.

In the future, we will explore more effective preservation and rejuvenation methods to maintain the stability of strain performance during long - term storage and passage. Meanwhile, the mechanism of strain performance degradation will be investigated to provide a theoretical basis for strain improvement and optimization. At the same time, protein engineering and other means will be utilized to modify lipase to enhance its performance to meet specific application requirements. By employing genomics, transcriptomics, proteomics and other multi - omics technologies, we will further study the molecular mechanism of high - level expression of lipase in strains under low - temperature conditions, and provide new ideas and methods for strain improvement and optimization. The production cost, process feasibility, product safety and other aspects of low - temperature lipase will be comprehensively evaluated to explore its industrial application potential in food processing, low - temperature washing, and environmental treatment.

## Conclusion

The demand for low-temperature lipase is increasing, and its application value in the fields of food preservation, low-temperature detergent development and environmental remediation continues to be highlighted. Especially in the context of the upgrading of the global cold chain

food industry and the tightening of green washing standards in the spring of 2026, the development of this enzyme has entered a critical window period. *Aspergillus niger* Y-A02 was successfully isolated from the soil of low-temperature forest and identified as *Aspergillus niger* Y-A02. The mutant strain Y-B04 with a 127.35% increase in lipase production was obtained by UV-NMG mutagenesis. By optimizing the fermentation conditions (temperature 21℃, pH 6.0, inoculum size $6.5\times10^6$ spores), the enzyme yield was further increased to 57.26 U/mL. The low-temperature lipase with a specific activity of 113.52 U/mg was successfully isolated and purified by ammonium sulfate precipitation, Q-HP anion exchange chromatography and Superdex 75 gel filtration chromatography. The optimum reaction temperature of the lipase was 30℃, and it showed excellent low-temperature adaptability. The temperature stability, pH tolerance, the effects of metal ions and organic solvents, substrate specificity and kinetic parameters of the low-temperature lipase were systematically studied. This study not only enriched the resource pool of low-temperature lipase producing bacteria, but also significantly improved the yield and performance of low-temperature lipase through mutation breeding, fermentation optimization, isolation and purification, which provided scientific basis and technical support for the industrial production of low-temperature lipase.

## Data availability

The original contributions presented in this study are included in the article. Further inquiries can be directed to the corresponding authors. The ITS gene sequence data for strain YLT-A02 is available in NCBI with accession PZ532477.

## Acknowledgements

We would like to express our sincere gratitude to Shanghai Personalbio Biotechnology Co., Ltd. for providing the sample sequencing and species identification services.

## Author contributions

Writing—original draft preparation and methodology, L.Y.; writing—reviewing and editing, M.W. and B.J.; visualization, H.F.and Y.Z.; data curation, Y.Z.; formal analysis, M.C.; validation, H.C.; funding acquisition, Y.C. All authors have read and agreed to the published version of the manuscript.

## Funding

Research Innovation Platform Research Project of the School of Food Engineering, East University of Heilongjiang (HDFSP250302A).

## Competing interests

The authors declare no conflicts of interest.

## References

1 Henrich, L. *et al.* Investigation of regioselectivity and thermostability of free and immobilized Pleurotus citrinopileatus lipase. *Applied microbiology and biotechnology* **110**, 134–134 (2026). https://doi.org/10.1007/s00253-026-13801-5

2 Gudiño, E. D., Iglesias, L. E. & Ferreira, M. L. A rational approach to the regioselective deacetylation of 2′,3′,5′-tri- O -acetyluridine by Novozym 435 catalysed alcoholysis. *BBA - Proteins and Proteomics* **1824**, 627–636 (2012). https://doi.org/10.1016/j.bbapap.2012.01.009

3 Nascimento, E. M. d., Voll, F. A. P., Krieger, N. & Mitchell, D. A. Homotropic allostery of Rhizomucor miehei lipase in the desymmetrization of diols: A note of caution. *Biochemical Engineering Journal* **232**, 110209–110209 (2026).

https://doi.org/10.1016/j.Bej.2026.110209
4 Bernard, L. *et al.* Feed restriction has no effect on milk lipolysis, although it results in a marked reduction in milk lipoprotein lipase activity in dairy goats. *Small Ruminant Research* **254**, 107649–107649 (2026). https://doi.org/10.1016/j.Smallrumres.2025.107649
5 Collaço, A. C. A., Aguieiras, E. C. G., Cavalcanti, E. D. C. & Freire, D. M. G. Development of an integrated process involving palm industry co-products for monoglyceride/diglyceride emulsifier synthesis: Use of palm cake and fiber for lipase production and palm fatty-acid distillate as raw material. *LWT* **135**, 110039– (2021). https://doi.org/10.1016/j.lwt.2020.110039
6 Sato, H., Ichikawa, K., Shiono, Y. & Koseki, T. Enzymatic degradation of γ-oryzanol and dibutyl phthalate by Aspergillus oryzae lipase. *Journal of bioscience and bioengineering* (2026). https://doi.org/10.1016/j.Jbiosc.2026.03.004
7 Adebami, G. E., Tayo, B. C. A., Kuila, A., Babalola, B. A. & Abiala, M. A. Biosourcing and optimization of fungal lipase production from cheap agro waste via solid state fermentation. *Scientific Reports* **15**, 20967–20967 (2025). https://doi.org/10.1038/s41598-025-06505-9
8 Qi, L. *et al.* A novel lipase from Aspergillus oryzae WZ007 catalyzed synthesis of brivaracetam intermediate and its enzymatic characterization. *Chirality* **33**, 62–71 (2020). https://doi.org/10.1002/chir.23286
9 He, B. *et al.* Gene Cloning, Purification, and Characterization of a Cold-Active Alkaline Lipase from Bacillus cereus U2. *Fermentation* **11**, 365–365 (2025). https://doi.org/10.3390/fermentation11070365
10 Yali, Z. *et al.* Melia azedarach leaf powder stabilizing Pseudomonas fluorescens lipase to catalyze synthesis of geranyl acetate. *Biocatalysis and Agricultural Biotechnology* **37** (2021). https://doi.org/10.1016/j.Bcab.2021.102170
11 Qiurun, M., Aili, L., Hailun, G., Yan, Z. & Mu, L. A novel thermostable and organic solvent-tolerant lipase from Xanthomonas oryzae pv. oryzae YB103: screening, purification and characterization. *Extremophiles : life under extreme conditions* **20**, 157–165 (2016). https://doi.org/10.1007/s00792-016-0809-y
12 Erkanli, M. E., Halabi, K. E., Kang, T. K. & Kim, J. R. Hotspot Wizard-informed engineering of a hyperthermophilic β-glucosidase for enhanced enzyme activity at low temperatures. *Biotechnology and bioengineering* **121**, 2079–2090 (2024). https://doi.org/10.1002/bit.28732
13 Ganasen, M. *et al.* Cold-adapted organic solvent tolerant alkalophilic family I.3 lipase from an Antarctic Pseudomonas. *International Journal of Biological Macromolecules* **92**, 1266–1276 (2016). https://doi.org/10.1016/j.ijbiomac.2016.06.095
14 Goomber, S., Kumar, A. & Kaur, J. Disruption of N terminus long range non covalent interactions shifted temp. opt 25°C to cold: Evolution of point mutant Bacillus lipase by error prone PCR. *Gene* **576**, 237–243 (2016). https://doi.org/10.1016/j.gene.2015.10.006
15 Balaei, F., Pouraghajan, K., Mohammadi, S., Ghobadi, S. & Khodarahmi, R. Enhancing Cryo-Enzymatic Efficiency in Cold-Adapted Lipase from Psychrobacter sp. C18 via Site-Directed Mutagenesis. *Archives of biochemistry and biophysics* **768**, 110388 (2025). https://doi.org/10.1016/j.Abb.2025.110388
16 Hua, L. *et al.* Selection and Genetic Analysis of High Polysaccharide-Producing Mutants in Inonotus obliquus. *Microorganisms* **12**, 1335–1335 (2024).

https://doi.org/10.3390/microorganisms12071335
17 TOIDA, J. Breeding of High Lipase Producing Strain from Aspergillus oryzae and its Usefulness for Miso Fermentation. *JOURNAL OF THE BREWING SOCIETY OF JAPAN* **106**, 457–461 (2011). https://doi.org/10.6013/jbrewsocjapan.106.457
18 Shreya, Bhati, N. & Sharma, A. Mutagenesis, purification, and characterization of lipase from Aspergillus eucalypticola CBS 122712 and exhibiting efficient removal of vehicle oil stains. *Bioresource Technology Reports* **20** (2022). https://doi.org/10.1016/j.biteb.2022.101228
19 Zhang, Z. *et al.* Soil Carbon Concentrations and Their Stability in the Active and Permafrost Layers of the Da Xing'an Mountains, Northeast China. *Permafrost and Periglacial Processes* **36**, 702–714 (2025). https://doi.org/10.1002/ppp.70002
20 Xing, C. *et al.* Screening of thermophilic neutral lipase producing Pseudomonas sp ZBC1 and improving its enzymatic activity. *African Journal of Biotechnology* **12** (2013).
21 Ali, M. S. M. *et al.* Cold-Adapted RTX Lipase from Antarctic Pseudomonas sp. Strain AMS8: Isolation, Molecular Modeling and Heterologous Expression. *The Protein Journal* **32**, 317–325 (2013). https://doi.org/10.1007/s10930-013-9488-z
22 Hasan, F., Shah, A. A. & Hameed, A. Methods for detection and characterization of lipases: A comprehensive review. *Biotechnology Advances* **27**, 782–798 (2009). https://doi.org/10.1016/j.biotechadv.2009.06.001
23 Yang, L., Shi, Y., Yang, B. & Wu, H. Preparation of lutein through biotransformation in a microemulsion medium. *Royal Society Open Science* **13** (2026). https://doi.org/10.1098/rsos.251373
24 L, S. C. *et al.* Nuclear ribosomal internal transcribed spacer (ITS) region as a universal DNA barcode marker for Fungi. *Proceedings of the National Academy of Sciences of the United States of America* **109**, 6241–6246 (2012). https://doi.org/10.1073/pnas.1117018109
25 Zhang, S. *et al.* Enhancing Pullulan Production inAureobasidium pullulansthrough UV Mutagenesis Breeding and High-Throughput Screening System. *Fermentation* **10**, 103– (2024). https://doi.org/10.3390/fermentation10020103
26 Lu, F. *et al.* Unveiling underlying mechanism of combined He–Ne laser and UV mutagenesis in Bacillus subtilis CICC 21927: A transcriptomic analysis. *Food Bioscience* **61**, 104694–104694 (2024). https://doi.org/10.1016/j.Fbio.2024.104694
27 Saranya, S. & Chellapandi, P. Comparative evaluation of chemical and UV mutagenesis with post-mutagenesis process optimization for enhanced cellulolytic enzyme production by Aspergillus oryzae NCIM 637. *Bioresource Technology Reports* **32**, 102349–102349 (2025). https://doi.org/10.1016/j.Biteb.2025.102349
28 Yao, B. *et al.* Enhanced Production, Purification, and Characterization of α-Glucosidase from NTG-Mutagenized Aspergillus niger for Industrial Applications. *Catalysts* **15**, 450–450 (2025). https://doi.org/10.3390/catal15050450
29 Goldbeck, R. & Filho, F. M. Screening, characterization, and biocatalytic capacity of lipases producing wild yeasts from Brazil biomes. *Food Science and Biotechnology* **22**, 79–87 (2013). https://doi.org/10.1007/s10068-013-0052-6
30 Yılmaz, D. E., Yalçın, H. T. & Sayar, N. A. Screening of Lipase Production Among Different Microorganisms. *New BIOTECHNOLOGY* **31**, S90–S90 (2014). https://doi.org/10.1016/j.nbt.2014.05.1821
31 Ronglin, H. *et al.* Mutagenesis and evaluation of cellulase properties and cellulose

hydrolysis of Talaromyces piceus. *World journal of microbiology & biotechnology* **31**, 1811–1819 (2015). https://doi.org/10.1007/s11274-015-1934-y

32 Ado, B. V., Dung, P. B. & Ichor, T. Temperature and pH-Driven Lipase Dynamics of Penicillium spp. and Aspergillus niger for Sustainable Treatment of Agro-industrial Wastewater. *South Asian Journal of Research in Microbiology* **19**, 76–92 (2025). https://doi.org/10.9734/sajrm/2025/v19i6444

33 Grintzalis, K., Georgiou, C. & Schneider, Y. An accurate and sensitive Coomassie Brilliant Blue G-250-based assay for protein determination. *Analytical Biochemistry* **480**, 28–30 (2015). https://doi.org/10.1016/j.ab.2015.03.024

34 Georgiou, C., Grintzalis, K., Zervoudakis, G. & Papapostolou, I. Mechanism of Coomassie brilliant blue G-250 binding to proteins: a hydrophobic assay for nanogram quantities of proteins. *Analytical and Bioanalytical Chemistry* **391**, 391–403 (2008). https://doi.org/10.1007/s00216-008-1996-x

35 Okut, C. B. A. & Türkhan, A. Purification and Biochemical Characterization of Polyphenol Oxidase from Falcaria vulgaris Bernh. †. *Molecules* **30**, 4806–4806 (2025). https://doi.org/10.3390/molecules30244806

36 Katragadda, M., Ingilala, V. & Kodali, V. P. Purification and characterization of a novel alkaline laccase produced by Acinetobacter sp. M6. *3 Biotech* **16**, 5–5 (2025). https://doi.org/10.1007/s13205-025-04622-w

37 Li, M. *et al.* Rapid purification and characterization of angiotensin I-converting enzyme from porcine lung. *Protein Expression and Purification* **235** (2025). https://doi.org/10.1016/j.pep.2025.106780

38 Yu, K. *et al.* Purification and Biochemical Characterization of Polyphenol Oxidase Extracted from Wheat Bran (Wan grano). *Molecules* **29** (2024). https://doi.org/10.3390/molecules29061334

39 Lee, S., Hwang, J., Choi, S. & Kim, S. Purification and characterization of Aspergillus oryzae LK-101 salt-tolerant acid protease isolated from soybean paste. *Food Science and Biotechnology* **19**, 327–334 (2010). https://doi.org/10.1007/s10068-010-0047-5

40 Gong, X. *et al.* The determination of dissociation constants for active ingredients from herbal extracts using a liquid liquid equilibrium method. *Fluid Phase Equilibria* **409**, 447–457 (2016). https://doi.org/10.1016/j.fluid.2015.11.004

41 Hafsa, K. *et al.* Screening, optimization, and molecular characterization of cold-active lipase producing Bacillus cereus I13 from Arctic sediments. *Biologia* **79**, 1041–1055 (2024). https://doi.org/10.1007/s11756-024-01610-y

42 Yu, P. *et al.* Characterization of Lactococcus lactis grx602: A novel lipase-producing probiotic strain for nutritional and sensory enhancement of sour cream. *Food Bioscience* **74**, 107918–107918 (2025). https://doi.org/10.1016/j.Fbio.2025.107918

43 Luo, Y. *et al.* Identification and characterization of Streptomyces sp. strain NEAU-174 with biocontrol ability against tomato bacterial wilt. *Physiological and Molecular Plant Pathology* **141**, 102985–102985 (2026). https://doi.org/10.1016/j.Pmpp.2025.102985

44 Adebali, O., Mieczkowski, P. A., Sancar, A. & Selby, C. P. Genome-wide strand-specific UV mutagenesis in Escherichia coli is directed by the Mfd translocase. *Proceedings of the National Academy of Sciences of the United States of America* **122**, e2523368122 (2025). https://doi.org/10.1073/pnas.2523368122

45 Song, K. *et al.* Screening, UV Mutagenesis, and Exploration of Enzymatic Degradation Mechanisms in the Highly Efficient Polyurethane-Degrading Bacillus sp. J-11. *Journal of*

*applied microbiology* (2025). https://doi.org/10.1093/jambio/lxaf224
46 Harper, M. & Lee, C. J. Genome-wide analysis of mutagenesis bias and context sensitivity of N-methyl-N′-nitro-N-nitrosoguanidine (NTG). *Mutation Research - Fundamental and Molecular Mechanisms of Mutagenesis* **731**, 64–67 (2012). https://doi.org/10.1016/j.mrfmmm.2011.10.011
47 Bo, Z. *et al.* Improvement of amphotericin B production by a newly isolated Streptomyces nodosus mutant. *Biotechnology and applied biochemistry* **65**, 188–194 (2018). https://doi.org/10.1002/bab.1579
48 Santos, C. J. D., Santos, R. D., Cerqueira, K. S., Rodrigues, J. R. S. & Souza, R. R. D. Production of free fatty acids by enzymatic hydrolysis of residual frying oil using non-commercial lipases from Aspergillus niger. *Anais da Academia Brasileira de Ciencias* **96**, e20240781 (2025). https://doi.org/10.1590/0001-3765202420240781
49 Idris, M. A., Ahmad, K. N. H., Chor, L. A. T., Nurbaya, O. S. & Mohamad, A. M. S. Cold-Active Lipases and Esterases: A Review on Recombinant Overexpression and Other Essential Issues. *International Journal of Molecular Sciences* **23**, 15394–15394 (2022). https://doi.org/10.3390/ijms232315394
50 Cao, X., Liao, L. & Feng, F. Purification and characterization of an extracellular lipase from Trichosporon sp. and its application in enrichment of omega-3 polyunsaturated fatty acids. *LWT* **118**, 108692–108692 (2020). https://doi.org/10.1016/j.lwt.2019.108692
51 Gulen, R. B., Ugur, A. & Sarac, N. Purification and Characterization of an Alkaline Lipase from Streptomyces sp. AU-153 and Evaluation of Its Detergent Compatibility. *ACS omega* **11**, 8470–8478 (2026). https://doi.org/10.1021/acsomega.5c11317
52 Liu, S. *et al.* Effects of nitrogen and carbon source addition on biomass and protein production by Rhodopseudomonas via the RSM-CCD approach. *Desalination and Water Treatment* **319**, 100438– (2024). https://doi.org/10.1016/j.Dwt.2024.100438
53 Shan, W. *et al.* Insights into the Underlying Mechanism of Ochratoxin A Production in Aspergillus niger CBS 513.88 Using Different Carbon Sources. *Toxins* **14**, 551–551 (2022). https://doi.org/10.3390/toxins14080551
54 Ali, I. *et al.* Statistical optimization of pectinases from thermophilic Aspergillus fumigatus BT-4 employing response surface methodology through submerged fermentation using agricultural wastes. *BMC Biotechnology* **25**, 1–1 (2025). https://doi.org/10.1186/s12896-024-00942-6
55 Pirjo, P., Timo, S., Taina, T. & Pirjo, N.-I. Preparation and Purification of β-1,3-glucan-Linked Candida glabrata Cell Wall Proteases by Ion-Exchange Chromatography, Gel Filtration, and MDPF-Gelatin-Zymography Assay. *Bio-protocol* **14**, e4958–e4958 (2024). https://doi.org/10.21769/bioprotoc.4958
56 Sangeetha, S. & Growther, L. Application of a two-level factorial design to investigate the effects of pH, temperature, nitrate concentration, and photoperiod on novel extracellular lipase activity of Nodosilinea sp. LGS3. *Journal of microbiological methods* **240**, 107354 (2025). https://doi.org/10.1016/j.Mimet.2025.107354
57 Lee, J., Lee, H., Kim, T. & Chang, P. S. In silico mining of sn-1,3 regioselective Rhizomucor miehei lipase homolog with strict pH sensitivity from Cordyceps militaris. *Food chemistry* **495**, 146653 (2025). https://doi.org/10.1016/j.Foodchem.2025.146653
58 N., S. *et al.* Metal ion type significantly affects the morphology but not the activity of lipase–metal–phosphate nanoflowers. *RSC Advances* **7**, 25437–25443 (2017). https://doi.org/10.1039/c7ra00302a

59 Jiale, L. *et al.* Biomimetic Mineralization of Metal Ion-Doped Lipase into ZIF-8 Framework for Enhanced Hydrolytic Activity in Biphasic System. *ChemistrySelect* **7** (2022). https://doi.org/10.1002/slct.202202721

60 Santos, J. C. B., Barbosa, M. S., Souza, R. L., Soares, C. M. F. & Pereira, M. M. Molecular dynamics elucidation of ion-dependent formation mechanisms in lipase hybrid nanoflowers. *Molecular Catalysis* **596**, 115922–115922 (2026). https://doi.org/10.1016/j.Mcat.2026.115922

61 Tjørnelund, H. D., Brask, J., Woodley, J. M. & Peters, G. H. J. Active Site Studies to Explain Kinetics of Lipases in Organic Solvents Using Molecular Dynamics Simulations. *The journal of physical chemistry. B* (2024). https://doi.org/10.1021/acs.Jpcb.4c05738

62 Dong, Z., Momeni, M. H., Olofsson, K. & Karlsson, E. N. Exploring the influence of lid region residues on fatty acid selectivity in a lipase originating from Rhizopus oryzae. *The FEBS journal* **293**, 878–893 (2025). https://doi.org/10.1111/febs.70284

# Tables

**Table 1.** Response Surface Test Factors and Levels

| Level | A Temperature(℃) | B pH | C Inoculum size(spore) |
|---|---|---|---|
| -1 | 15 | 5 | $4\times10^6$ |
| 0 | 20 | 6 | $6\times10^6$ |
| 1 | 25 | 7 | $8\times10^6$ |

**Table 2.** Lipase activity before and after compound mutagenesis

| Strain number | Colony diameter (cm) | Fluorescence circle diameter (cm) | Ratio of fluorescence circle diameter to colony diameter (D/d) | Lipase activity (U/mL) |
|---|---|---|---|---|
| Y-A02 | 1.22 | 1.54 | 1.26 | 21.50±1.54 |
| Y-B01 | 1.34 | 2.33 | 1.74 | 46.74±2.13 |
| Y-B02 | 1.36 | 2.45 | 1.80 | 48.23±1.76 |
| Y-B03 | 1.27 | 2.12 | 1.67 | 45.49±1.31 |

| | | | | |
|---|---|---|---|---|
| Y-B04 | 1.38 | 2.47 | 1.86 | 48.88±1.94 |
| Y-B05 | 1.27 | 2.04 | 1.61 | 44.72±2.52 |
| Y-B06 | 1.23 | 1.91 | 1.55 | 43.26±2.04 |
| Y-B07 | 1.03 | 1.75 | 1.70 | 44.06±2.81 |
| Y-B08 | 1.15 | 1.84 | 1.60 | 41.22±2.13 |
| Y-B09 | 1.24 | 1.88 | 1.52 | 40.73±1.87 |
| Y-B10 | 1.11 | 1.93 | 1.74 | 47.12±1.74 |
| Y-B11 | 1.27 | 2.29 | 1.80 | 47.81±2.33 |
| Y-B12 | 1.26 | 2.17 | 1.72 | 46.26±1.84 |
| Y-B13 | 1.17 | 1.96 | 1.68 | 45.55±2.01 |
| Y-B14 | 1.44 | 2.53 | 1.76 | 47.12±1.85 |
| Y-B15 | 1.28 | 2.27 | 1.77 | 47.37±1.49 |

963 **Table 3.** Results of genetic stability of mutant strains

| Number | Lipase activity（U/mL） | | | | |
|---|---|---|---|---|---|
| | 1 | 2 | 3 | 4 | 5 |
| Y-B02 | 48.27±1.65 | 47.31±2.16 | 47.11±1.26 | 47.76±3.11 | 43.02±1.47 |
| Y-B04 | 48.45±1.47 | 49.46±1.27 | 50.21±2.21 | 48.67±1.53 | 49.33±2.07 |
| Y-B11 | 47.66±2.26 | 47.17±2.81 | 46.42±3.01 | 47.11±2.26 | 47.13±2.32 |
| Y-B14 | 46.71±1.87 | 47.16±1.68 | 45.28±2.54 | 44.25±1.41 | 41.03±3.41 |
| Y-B15 | 47.27±2.16 | 47.52±2.01 | 47.61±1.70 | 48.02±1.71 | 48.12±3.41 |

964 **Table 4.** Response Surface Test Design and Results

| Number | A Temperature(℃) | B pH | C Inoculum size(spore) | Lipase activity （U/mL） |
|---|---|---|---|---|
| 1 | 15 | 5.0 | $6\times10^6$ | 46.69 |
| 2 | 25 | 5.0 | $6\times10^6$ | 50.72 |
| 3 | 15 | 7.0 | $6\times10^6$ | 48.68 |
| 4 | 25 | 7.0 | $6\times10^6$ | 50.12 |
| 5 | 15 | 6.0 | $4\times10^6$ | 43.59 |
| 6 | 25 | 6.0 | $4\times10^6$ | 44.47 |
| 7 | 15 | 6.0 | $8\times10^6$ | 46.57 |
| 8 | 25 | 6.0 | $8\times10^6$ | 51.79 |
| 9 | 20 | 5.0 | $4\times10^6$ | 46.75 |
| 10 | 20 | 5.0 | $4\times10^6$ | 44.68 |
| 11 | 20 | 7.0 | $8\times10^6$ | 50.52 |
| 12 | 20 | 7.0 | $8\times10^6$ | 48.86 |
| 13 | 20 | 6.0 | $6\times10^6$ | 57.22 |
| 14 | 20 | 6.0 | $6\times10^6$ | 57.76 |
| 15 | 20 | 6.0 | $6\times10^6$ | 56.94 |
| 16 | 20 | 6.0 | $6\times10^6$ | 58.46 |
| 17 | 20 | 6.0 | $6\times10^6$ | 58.12 |

965 **Table 5**. Test results of regression simulation coefficient

| Source | Sum of Squares | df | Mean Square | F-value | P-value | Significance |
|---|---|---|---|---|---|---|
| Model | 424.35 | 9 | 47.15 | 59.12 | < 0.0001 | ** |
| A-Temperature | 16.73 | 1 | 16.73 | 20.98 | 0.0025 | ** |

| | | | | | | |
|---|---|---|---|---|---|---|
| B-pH | 0.6844 | 1 | 0.6844 | 0.8583 | 0.3851 | |
| C-Inoculum size | 41.63 | 1 | 41.63 | 52.21 | 0.0002 | ** |
| AB | 1.68 | 1 | 1.68 | 2.10 | 0.1903 | |
| AC | 4.71 | 1 | 4.71 | 5.90 | 0.0454 | * |
| BC | 0.0420 | 1 | 0.0420 | 0.0527 | 0.8250 | |
| $A^2$ | 99.96 | 1 | 99.96 | 125.35 | < 0.0001 | ** |
| $B^2$ | 60.00 | 1 | 60.00 | 75.24 | < 0.0001 | ** |
| $C^2$ | 163.03 | 1 | 163.03 | 204.43 | < 0.0001 | ** |
| Residual | 5.58 | 7 | 0.7975 | | | |
| Lack of Fit | 4.02 | 3 | 1.34 | 3.42 | 0.1329 | |
| Pure Error | 1.57 | 4 | 0.3914 | | | |
| Cor Total | 429.93 | 16 | | | | |

966 Note: ** indicates a highly significant difference ($P < 0.01$); * indicates a significant difference
967 ($P < 0.05$)

968 **Table 6.** Purification Table of Lipase

| Purification steps | Total activity (U) | Total protein (mg) | Specific Activity (U/mg) | Fold | Yield (%) |
|---|---|---|---|---|---|
| crude lipase | 15622.4 | 2196.1 | 7.11 | 1.00 | 100 |
| $(NH_4)_2SO_4$ fractional precipitation | 3221.6 | 173.6 | 18.54 | 2.61 | 20.62 |
| Q-HP | 1077.24 | 26.46 | 40.71 | 5.73 | 6.90 |

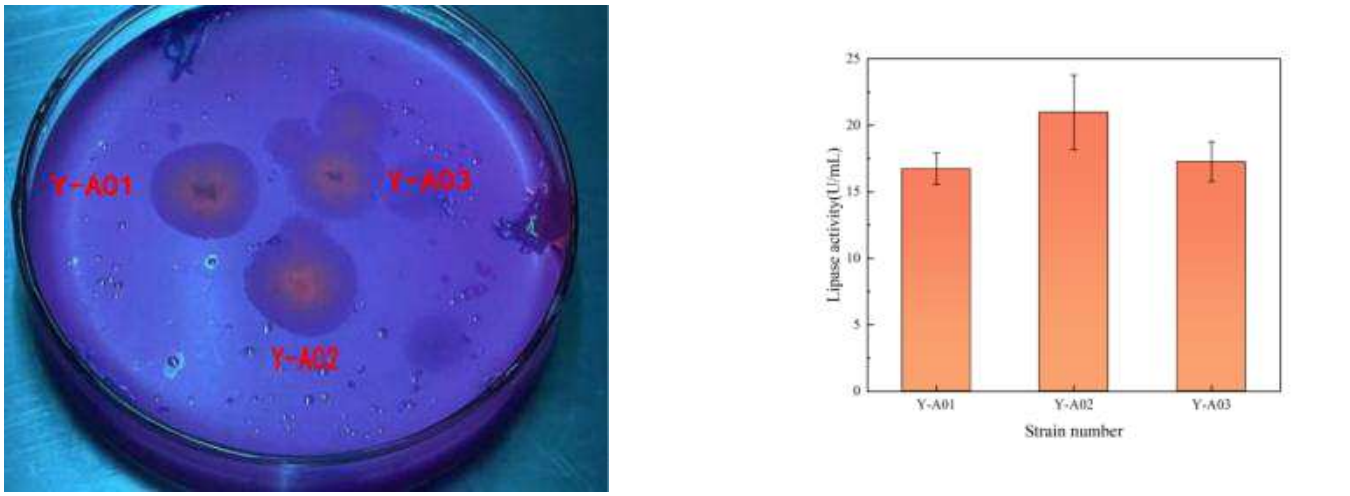
| | | | | | |
|---|---|---|---|---|---|
| Superdex 75 | 280.39 | 2.47 | 113.52 | 15.97 | 1.79 |

969 **Table 7.** Substrate selectivity of purified lipase

| Substrate name | Relative lipase activity(%) |
|---|---|
| p-NPC2 | 22.15±2.71 |
| p-NPC4 | 32.97±2.83 |
| p-NPC6 | 38.72±5.52 |
| p-NPC8 | 100±3.17 |
| p-NPC10 | 77.04±1.36 |
| p-NPC12 | 62.07±1.07 |
| p-NPC14 | 45.90±2.40 |
| p-NPC16 | 21.76±1.58 |
| p-NPC18 | 25.48±2.03 |

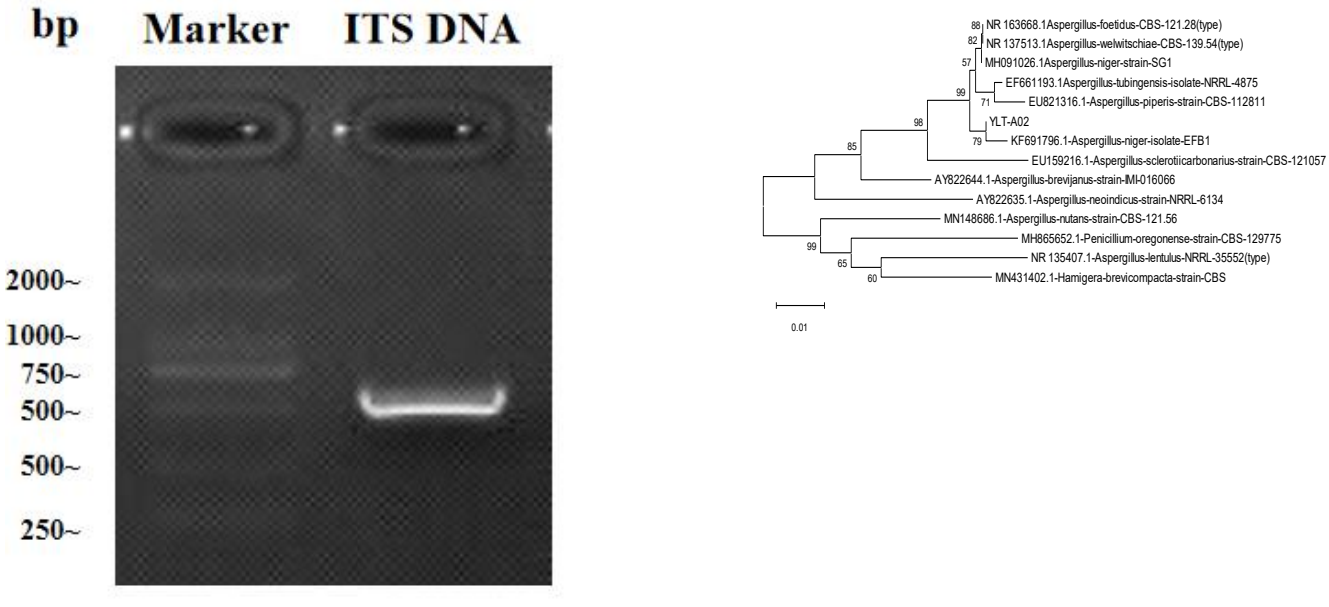
970

971 **Figures**



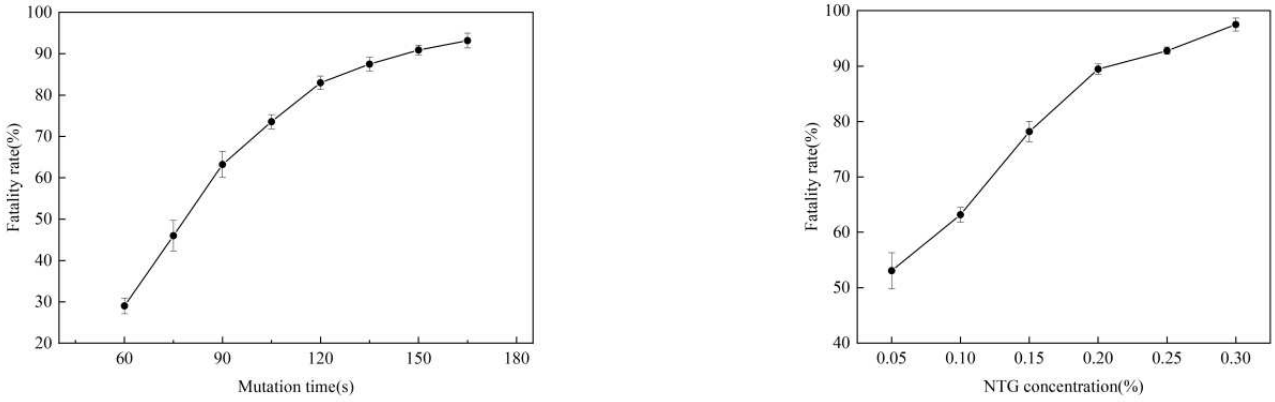

**(a)** **(b)**

972 **Figure 1.** Comparison of lipase-producing ability of three strains: (a) Rhodamine B lipid
973 screening medium fluorescence circle comparison, (b) Lipase activity assay of the strains



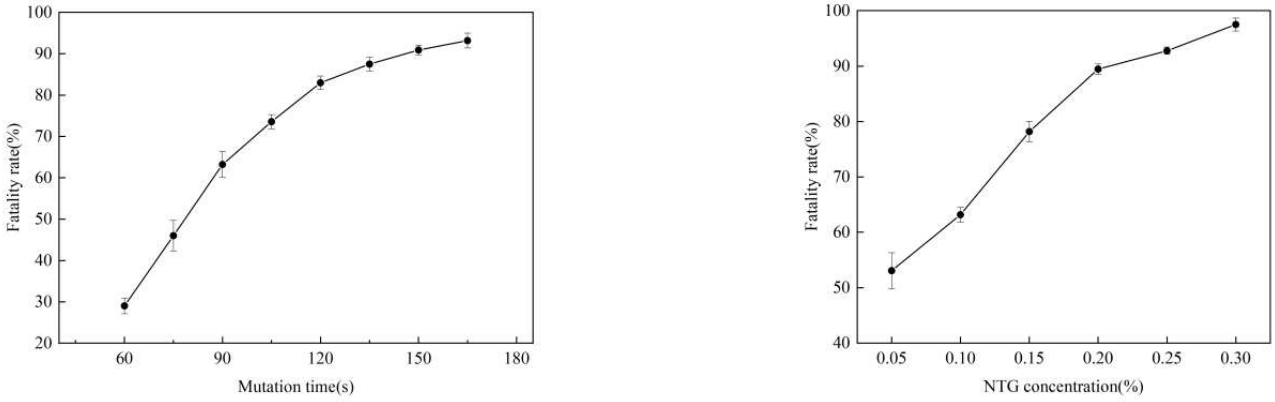

**(a)** **(b)**

974 **Figure 2.** Identification of strain Y-A02: (a) Electrophoresis results of strain Y-A02, (b)
975 phylogenetic tree of strain Y-A02



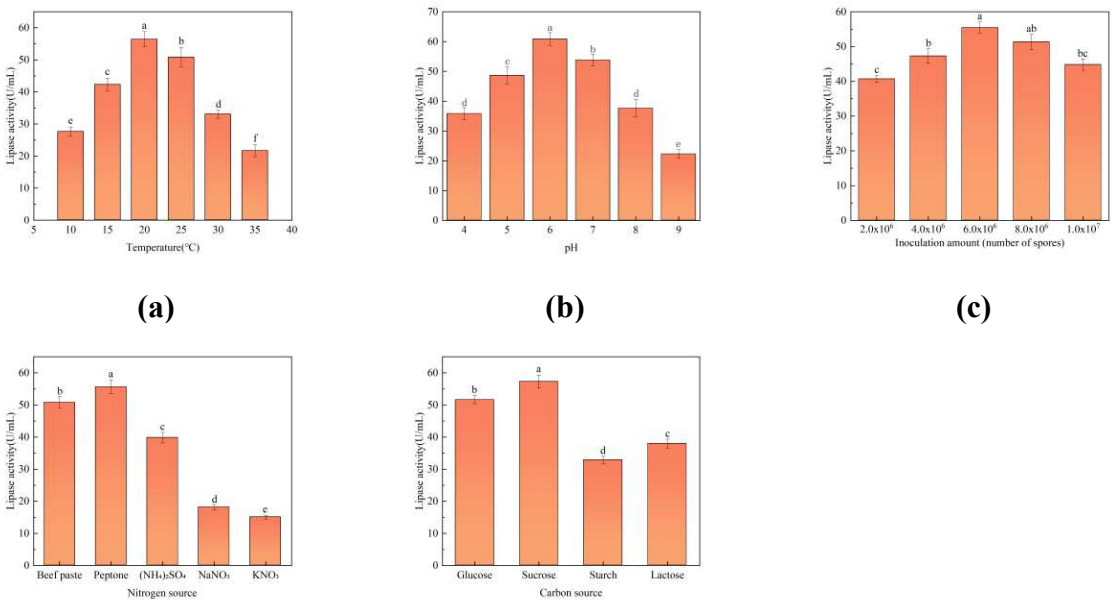

**(a)** **(b)**

976 **Figure 3.** Mutagenic lethality curves: (a) UV-induced lethality curves, (a) nitrosoguanidine
977 induced lethality curves

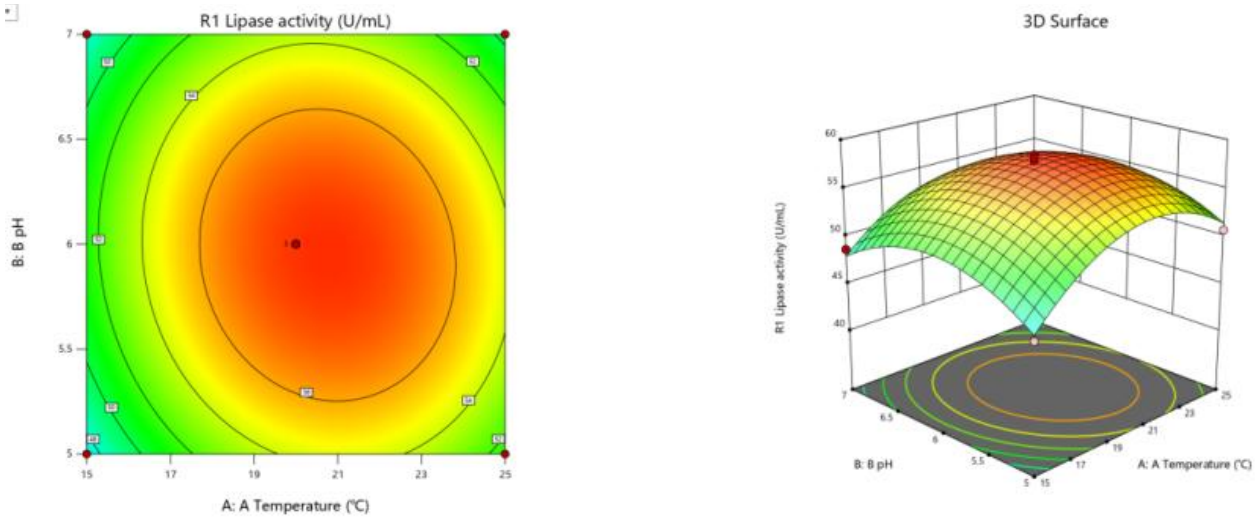



**(a)** **(b)**

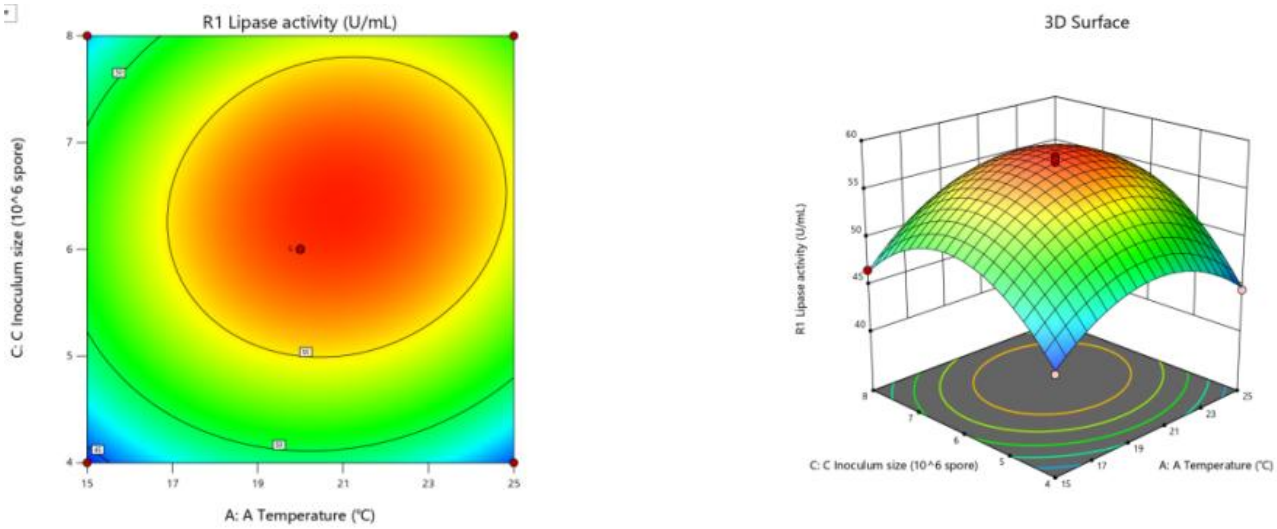
978 **Figure 4.** Comparison of fluorescent rings of the mutant strain Y-A02 (Fig.a) and the
979 mutant strain Y-B04 (Fig.b)



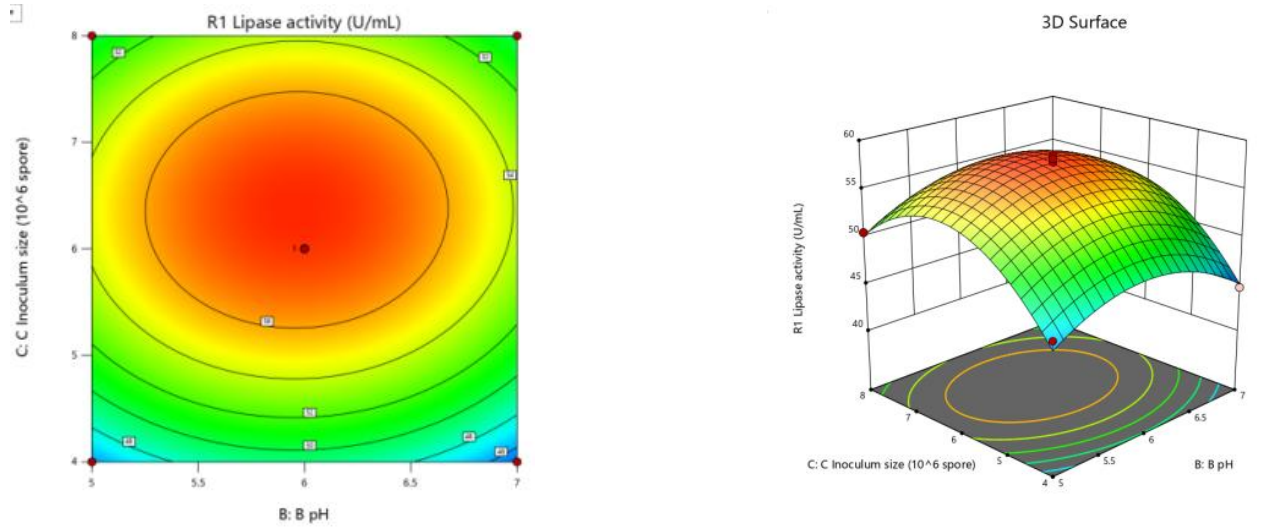

980 **Figure 5.** Optimization results of lipase production by liquid fermentation: (a) Effect of
981 temperature on lipase production, (b) Effect of pH on lipase production, (c) Effect of inoculum
982 size on lipase production, (d) effect of nitrogen source on lipase production, (e) Effect of carbon
983 source on lipase production



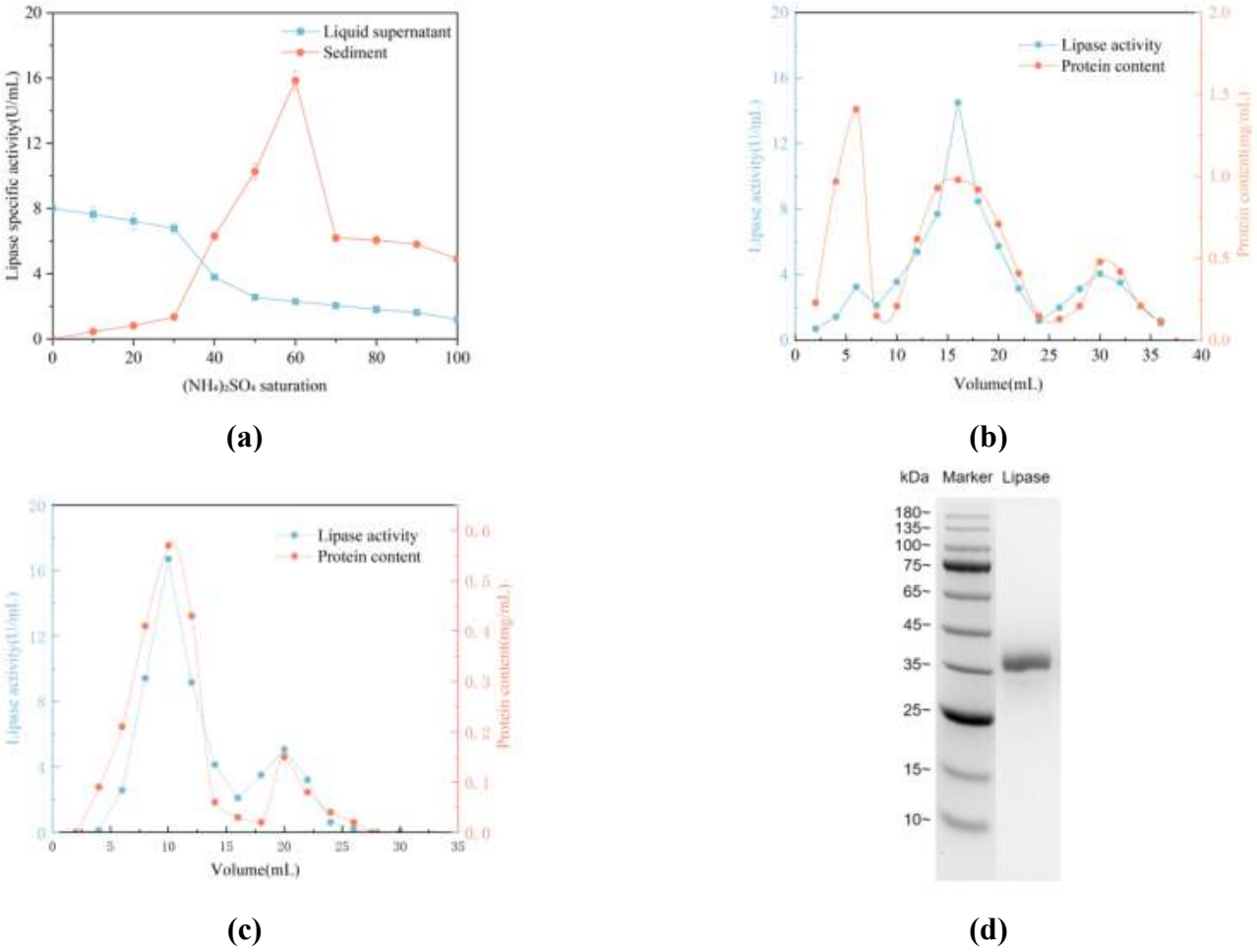

984 **Figure 6.** Response surface and profile of the interaction between factor A and factor B




985 **Figure 7.** Response surface and profile of the interaction between factor A and factor C

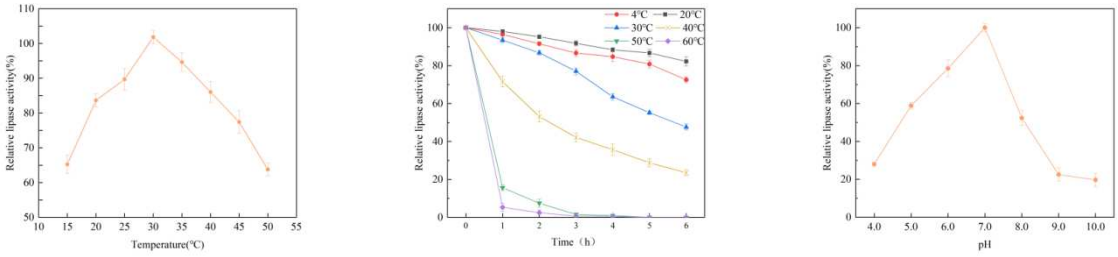


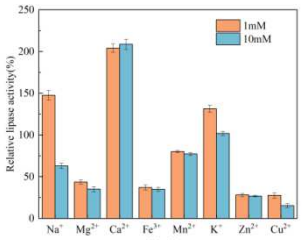

986 **Figure 8.** Response surface and profile of the interaction between factor B and factor C



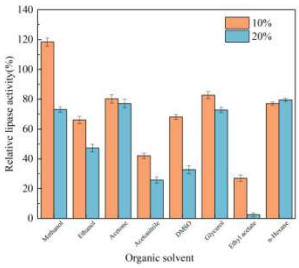

987 **Figure 9**. Isolation and purification of lipase: (a) $(NH_4)_2SO_4$ Salting out curve, (b) Q-HP elution

988 curve of lipase, (c) Superdex 75 elution curve of lipase, (d) SDS-PAGE analysis of lipase



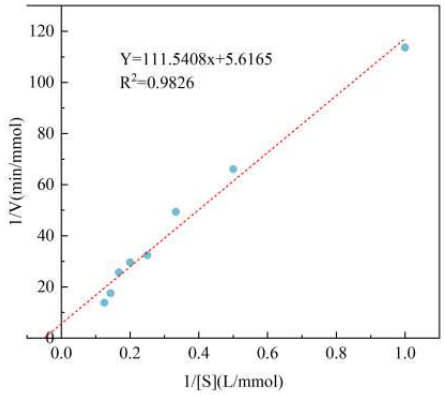



(d)




(e)

989 **Figure 10.** Investigation of the Enzymatic Properties of Lipase: (a) Appropriate reaction
990 temperature, (b) Temperature stability, (c) Appropriate reaction pH, (d) Effect of metal ions, (e)
991 Effects of organic solvents




992 **Figure 11.** The Lineweaver-Burk plot of lipase hydrolysis

993

## Supplementary Files

This is a list of supplementary files associated with this preprint. Click to download.

- Electrophoresis.zip